DC

Simulated and Measured Response of Robust Multilayer X-Ray Reflectors

A Dissertation

Presented to the

Department of Physics and Astronomy

Brigham Young University

In Partial Fulfillment

of the Requirements for the Degree

Doctor of Philosophy

by

Kevin J. Gray

August 1989

This Dissertation, by Kevin J. Gray, is accepted in its present form by the Department of Physics and Astronomy of Brigham Young University as satisfying the dissertation requirement for the degree of Doctor of Philosophy.

Larry V. Knight, Committee Chairman

David D. Allred, Committee Member

William E. Dibble, Committee Member

July 6, 1989

Date

Daniel L. Decker, Department Chairman

Simulated and Measured Response of Robust

Multilayer X-Ray Reflectors

ABSTRACT

Some recently proposed applications of multilayer x-ray reflectors expose the multilayer to damaging fluxes of x rays. This work reviews proposed damage mechanisms and material selection techniques aimed at reducing the effects of damaging fluxes. Experiments were performed to measure the response of tungsten/carbon, and tungsten carbide/carbon multilayers to laser plasma x-ray fluxes of approximately 200 MW/cm^2. These multilayers were found to maintain significant reflectivity for at least 1 ns. A computer program ROMULS has been developed which will predict the reflectivity vs. angle vs. time behavior of multilayers in high flux applications. A description of this program is given. Comparison of the simulations and experimental results indicate that ROMULS underestimates the useful lifetime of multilayers by a factor of two or three. Suggestions for improvements in experimental and simulation techniques are given. A detailed guide for operation of ROMULS is presented.

Table of Contents

List of Figures

Acknowledgments

I wish to thank the members of my committee for their guidance, especially Larry Knight and Jim Thorne for their direction in this work. I also am deeply indebted to Bryan Peterson for sharing his knowledge and skills.

I thank Lawrence Livermore National Laboratory and the Phoenix laser staff for the use of their facilities where these experiments were performed and Sam Thompson of Sandia National Laboratory for his assistance with the CHARTD code. Thanks also to Troy Barbee for providing the multilayers used in these experiments.

Finally, I wish to thank my family for their patience, understanding, and support, and for always being excited when daddy comes home.

This work was supported by Lawrence Livermore National Laboratory under Subcontract # 7330905.

I. INTRODUCTION

For many years after the discovery of x rays the only means available to reflect x rays were natural crystals and grazing incidence reflection. Early attempts at reflection of x rays by DuMond and Youtz[1] using synthetic structures were limited by large layer thicknesses and diffusion induced loss of reflectivity. With the adaptation of techniques used in the semiconductor industry it became possible to fabricate smaller, better, multilayered, x-ray reflectors (also known as layered synthetic microstructures or LSM's) of more favorable materials. Over the past fifteen years the technology to fabricate synthetic multilayered x ray reflectors has progressed to the point where their use is common. In addition to their use as reflectors multilayers have been exploited to form transmission gratings,[2] beam splitters,[3] and focusing optics.[4] Multilayers are now being used in devices recently seen only in the near visible region such as laser cavities,[5] monochromators,[6] and interferometers.[7]

A multilayer x-ray reflector is composed of alternating layers (on the order of tens of angstroms thick) of materials such as tungsten and carbon. Note that multilayers are commonly designated by the chemical symbols of their constituent materials, for example, tungsten carbide/carbon is designated WC/C. A typical multilayer will have between 30 and 100 layer pairs. X rays incident on the multilayer structure at an angle θ measured from grazing incidence will be reflected subject to the Bragg condition:

$$2d\sin\theta = \mathrm{m}\lambda \tag{1}$$

where d is the combined thickness of a pair of adjacent layers, m is the Bragg diffraction order, and λ is the wavelength of the incident x rays. Bragg's law as stated in equation (1) assumes an index of refraction of unity. The index of refraction in the

x-ray region is given by $n = 1 - \delta - i\beta$ where δ and β are small parameters known respectively as the index decrement and absorption index. Correction of Bragg's law for refractive effects resulting from a nonzero δ yields

$$2d\sin\theta = m\lambda\left(1 + \frac{\delta}{\sin^2\theta}\right). \tag{2}$$

Although Bragg's law enables determination of the angle at which x rays will be reflected it gives no information regarding the expected reflectivity of a given multilayer structure. The reflectivity is most readily calculated by computer since it involves the Fresnel coefficients for each interface in the structure. Reflectivity for an optimized multilayer can be as high as 90%. For a more detailed background on multilayers see Barbee[8] and Underwood and Atwood.[9]

Some of the applications of multilayers involve damaging fluxes of x rays thus the survivability of multilayers is an important issue. Several groups have demonstrated that multilayers are degraded by thermally activated mechanisms. Golub *et al.*,[10] observed increases in the *d*-spacing of ReW/C and V/C multilayers after annealing at 400°C for four hours. Ziegler *et al.*,[11] report loss of reflectivity in WRe/C and W/C multilayers due to crystallization after annealing at approximately 700°C. Thermal damage mechanisms are also present in non-refractory materials. In a similar study of Mo/Si multilayers Nakajima *et al.*,[12] observed loss of reflectivity and decrease in *d*-spacing after annealing at about 800°C. While these results are for annealing times on the order of minutes or hours they do give cause for concern in high flux applications such as plasma diagnostics and x-ray laser cavity mirrors where considerably higher temperatures are possible.

The success of an experiment may require that the multilayer maintain reflectivity for a predetermined time. Alternatively one may wish to maximize the

time over which experimental observations are possible by optimizing the multilayer design. In either case it is necessary to know how the multilayer can be expected to perform in a given experimental environment. This information may be obtained experimentally, but measurements of this type are not easily made. A simulation could be used in place of measurements if the predictions of the code were normalized to experiments. The purpose of this research was to model the effects of large, pulsed fluxes on the performance of multilayers, measure the response of multilayers under such conditions, and use the experimental results to validate the simulations.

The remainder of this work will consist of the following: Section II will describe the damage mechanisms expected to occur in pulsed flux situations and mechanisms which have actually been observed. Material selection techniques designed to limit the effects of these damage mechanisms will also be treated along with recommendations for general-use multilayer material pairs. In section III a description of experiments to measure the reflectivity vs. time response of V/C, W/C, and WC/C multilayers will be given. The results of these experiments will be discussed along with information they give regarding damage mechanisms. In section IV a computer program, ROMULS, will be described which predicts the reflectivity of a multilayer in pulsed applications. The results of simulations of the experimental conditions in the above described experiments will be presented along with the results of simulations of characterization experiments performed by other groups. Section IV also compares the results of these simulations with experiment and discusses possible causes for discrepancies. Finally, section V presents suggestions for improvements in the current work as a basis for future work. The appendices contain a user's manual for ROMULS.

II. DAMAGE MECHANISMS AND MATERIAL SELECTION

With increasing x-ray flux in multilayer applications there is increasing concern over the effects of absorbed energy on the multilayer. Many damage mechanisms have been predicted and some of these have been observed. The most obvious problem occurs when the flux is sufficiently high to cause phase transitions in the multilayer. Metal materials such as tungsten or vanadium may melt and intermix while carbon may vaporize. This effect may be catastrophic if the vapor pressure is sufficient to delaminate the structure. Melting was first observed by Kohler *et al.*,[13] in W/C multilayers.

As with the first metal multilayers diffusion may become a problem as the temperature of the multilayer increases. The diffusion times may be much shorter, however, because of the higher temperatures involved. Interdiffusion of the multilayer materials results in a loss of the sharp index of refraction gradient required for good reflectivity.

Another effect is a result of the non-equilibrium processes by which multilayers are fabricated. Examples of such processes are sputtering and evaporation. In either case the films are produced by rapid quenching of gas phase species and the resultant amorphous film is metastable. It is likely that due to heating of the multilayer there would be enough energy available to drive the crystallization process. For fast, pulsed applications crystallization is not likely for most materials because of the limited time. Rapid, sub-millisecond crystallization, also known as explosive crystallization, however, may be possible. Although it has not been observed in multilayers, silicon is known to exhibit this phenomena. It should be noted

that explosive crystallization of silicon in multilayers probably does not occur since Mo/Si is a common multilayer material pair and the effect has not been reported. Crystallization over time scales of hours has been observed in W/C, WRe/C, and other multilayers by Ziegler[11] and in Mo/Si by Nakajima.[12] In these experiments multilayers were annealed at temperatures near 400°C for several hours and their reflectivity after annealing was compared to before annealing. In all cases the multilayers showed comparatively little reflectivity subsequent to heating. Ziegler[11] did not, however, observe formation of tungsten carbide (W_2C) at the W/C interfaces as was reported by Tagaki[14] and as would be expected. Crystallization of amorphous layers and interfacial reactions are of great concern to those wishing to use multilayers in monochromator stages of synchrotron sources because of the inherent extended operation at elevated temperatures.

An effect which is not related directly to the x-ray flux but rather to the environment in which such fluxes are produced is plasma damage. For example large x-ray fluxes are often produced by laser plasma or plasma discharge techniques. The hot, dense plasmas produced in such experiments are known to damage any fragile structure in the vicinity by high energy ion bombardment. In fact in some experiments the majority of the damage is done by plasma bombardment (often referred to as plasma blowoff). An example of this is the x-ray laser cavity experiments at LLNL.[5] While it is likely that a great deal of damage was done to the multilayer by the large fluxes produced, it is evident from the damaged multilayers that large areas have been stripped off by the plasma leaving the bare substrate. An example of this type of damage can be seen in Figure 1. Fortunately, however, this damage often occurs long after the phenomenon of interest have ended because the plasma expands at a speed much less than the speed of light.

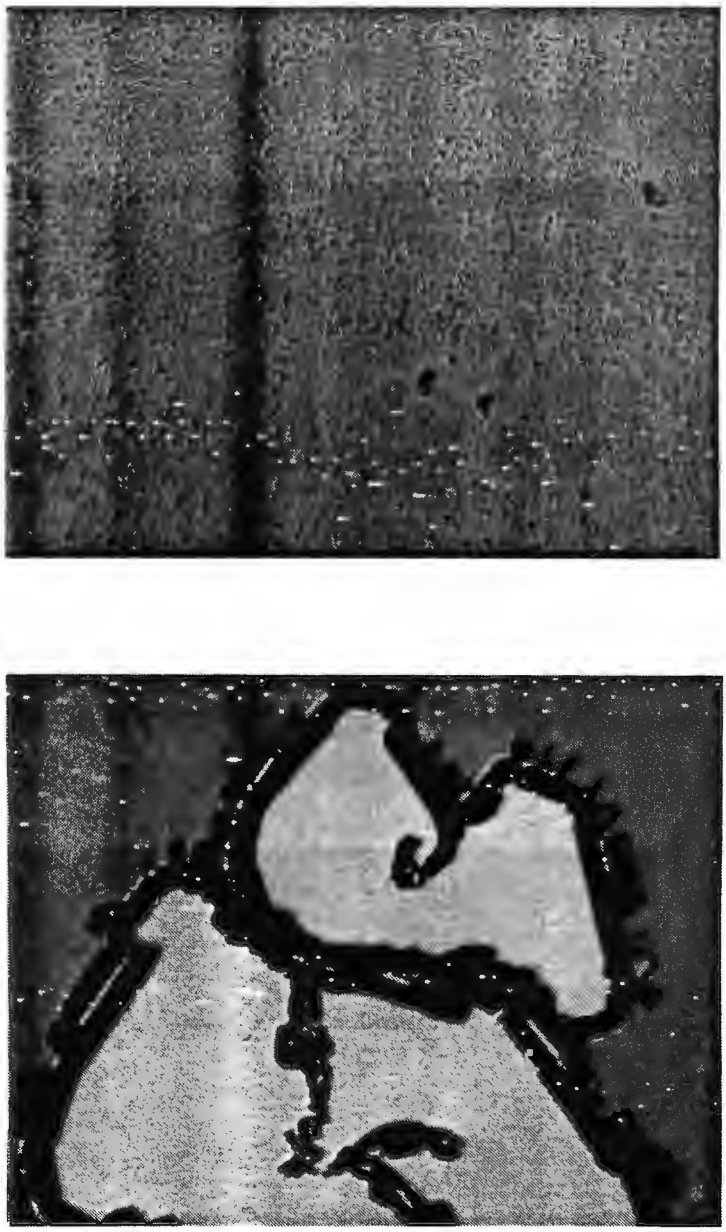

Figure 1. Example of a W/C multilayer which was damaged by plasma blowoff during characterization experiments. The upper micrograph (magnified 108 X) is of a part of the multilayer which was protected from the blowoff by a Be foil. These are Nomarski interferograms; the dark spots are blisters, not pits.

Finally, there is the possibility that the multilayer may be destroyed by induced thermal stresses. As the temperature in the multilayer increases, stresses will be induced at the interfaces if the thermal expansion coefficients differ. Although the bonds at the interfaces should be sufficiently strong to prevent slippage the induced stresses may cause bending of the multilayer. This type of damage may be especially important when considering free-standing multilayers or multilayers on extremely thin substrates.

When attempting to design a multilayer to withstand the fluxes and environments in many applications the above mentioned damage effects must be considered. It is therefore important that materials are chosen to minimize these effects. Such design considerations are treated in detail in reference 15. Briefly, materials are evaluated for maximum specific melt energy, that is, the energy required to melt one gram of the material. Next the phase diagrams of candidate material pairs must be examined to eliminate pairs with significant mutual solubility. Then the remaining possibilities are further narrowed by comparing relative electron densities. In order to have good reflectivity a multilayer must be composed of materials with different electron densities or a very large number of layers must be used. The latter has the advantage of greater resolution provided that the absorption in the materials allows for the required number of layers. Too large a difference in electron densities leads to reflection from only a few layers with a resultant poor resolution. Hopefully, a material pair can be found which has good reflectivity and resolution. Finally, the practical requirements of fabrication must be considered. Relevant questions are the availability of sputtering targets or the possibility of another fabrication technique such as chemical vapor deposition. Environmental or occupational hazards associated with the material and the cost of

fabrication must also be considered.

The results of the analysis given in reference 15 are that good general choices for robust multilayers are B_4C/C and TaC/C. Other multilayers may be superior for a specific application but these must be custom designed. It should be noted that another promising candidate is the B/vacuum multilayer. It may be possible[16] to deposit alternating layers of boron and an etchable material by chemical vapor deposition. After deposition the multilayer is etched leaving the boron layers separated by non-etched columns of the etchable material. As a comparison Figures 2, 3, and 4 compare these three multilayers optimized for reflectivity in the same application.

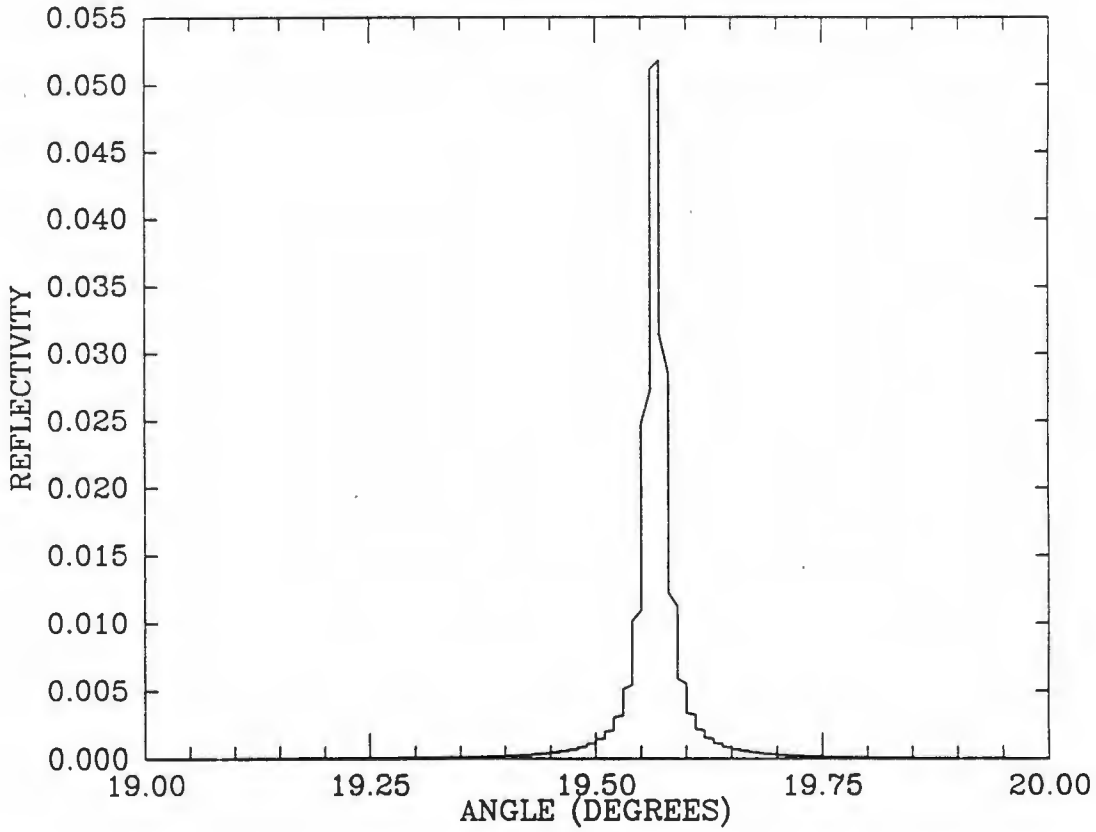

Figure 2. Calculated reflectivity versus angle at 13.33 Å of a B_4C/C multilayer with 2000 layer pairs and a d-spacing of 20.0 Å.

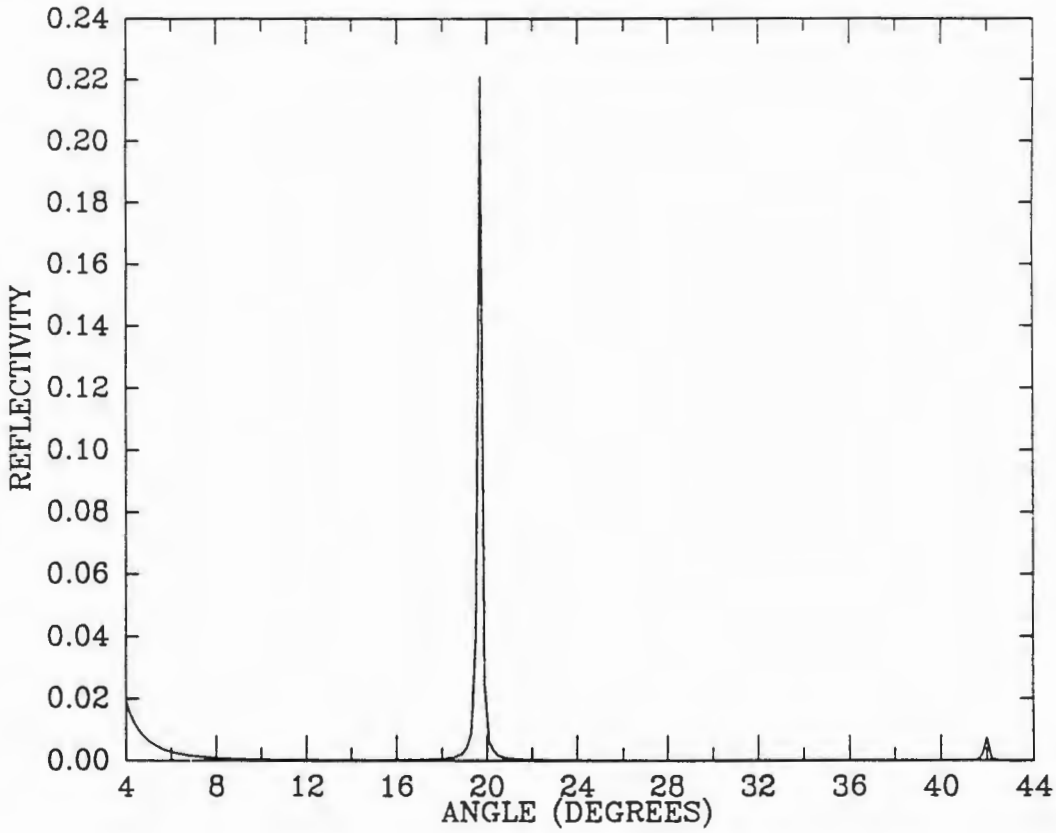

Figure 3. Calculated reflectivity versus angle at 13.33 Å of a TaC/C multilayer with 150 layer pairs and a *d*-spacing of 20.0 Å.

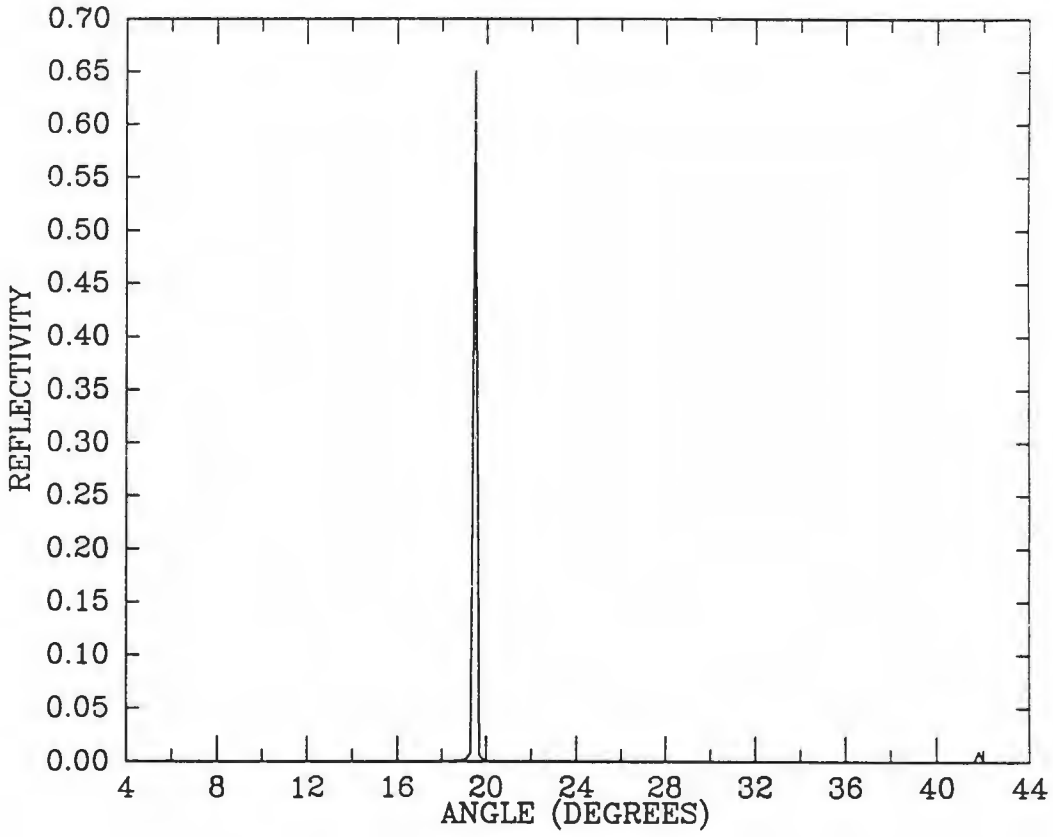

Figure 4. Calculated reflectivity versus angle at 13.33 Å of a B/vac multilayer with 500 layer pairs and a d-spacing of 20.0 Å.

III. EXPERIMENTAL CHARACTERIZATION OF MULTILAYERS

Once materials have been chosen according to the application and intended wavelength of use it is desirable to have some indication of how the multilayer can be expected to perform. Indeed many applications require detailed knowledge of the multilayer response. In any case the multilayer design will need to be tested and optimized. This information can be obtained either by a simulation or by experimental characterization. Direct measurements of multilayer response are conceptually simple but present many experimental difficulties since sufficiently bright sources, such as laser plasmas or spark generators, involve complex equipment. Furthermore, time resolved detectors such as x-ray diodes or x-ray streak cameras must be used.

A. Previous damage studies

Prior to our experiments, pulsed, high-flux damage studies were reported by three groups. First, a group at Lockheed (Kohler *et al.*,[13]) exposed W/C multilayers to a 20 ns pulse of x rays generated by a laser plasma and observed damage at a fluence level of about 0.5 J/cm^2. Ceglio *et al.*,[5] observed that Mo/Si multilayers used to form an x-ray laser cavity survived the initial x-ray flux but were later destroyed by plasma blow-off. More comprehensive experiments by Hockaday *et al.*,[17] employed a Z-pinch plasma source to expose W/C multilayers to large fluences. Hockaday observed [18] that one multilayer showed a drastic drop in reflectivity after exposure to an integrated flux of 2.5 J/cm^2 while a similar multilayer in another shot [19] displayed a similar loss of reflectivity after exposure to an integrated flux of 1.2 J/cm^2. In both of these cases the multilayers were irradiated for approximately 70 ns but the reflectivity losses were seen at 28 ns and 19 ns respectively. Loss of

reflectivity in these experiments was claimed to be due to melting of the tungsten layers.

B. Phoenix damage experiments

In our measurements of the response of multilayers to damaging fluxes we employed two laser plasmas as x-ray sources. These were generated by the Phoenix laser facility at Lawrence Livermore National Laboratory (LLNL). Phoenix is a two beam Nd:Glass laser with each beam providing approximately 25 J of 532 nm light in 750 ps pulses. The timing of the two beams relative to each other is controllable to within 200 ps which is the temporal resolution of the oscilloscope used to compare the signal from each beam. Precisely calibrated cables (length determined to within a few ps) are provided for synchronization of the laser pulses with streak cameras or other time resolved detectors.

A photograph of the target chamber room can be seen in Figure 5. The beams enter the room through the red "paddles" on the left of the room about half way up the wall. Optics on three small tables reflect the infrared beams through the two KDP frequency doubling crystals mounted near the entrance windows in the large black holders on the left and right side of the target chamber. The entrance optics focus the 4 inch diameter beams onto bulk Cu targets to produce the plasmas.

The concept of our experiments is depicted in Figure 6. One laser plasma was produced about 2 cm from the multilayer as a source of damaging x rays. A second plasma generated x rays incident on the multilayer at the Bragg angle as a probing source. X rays reflected from the multilayer impinged on the photocathode slit of an x-ray streak camera detector. The experimental sequence involved three

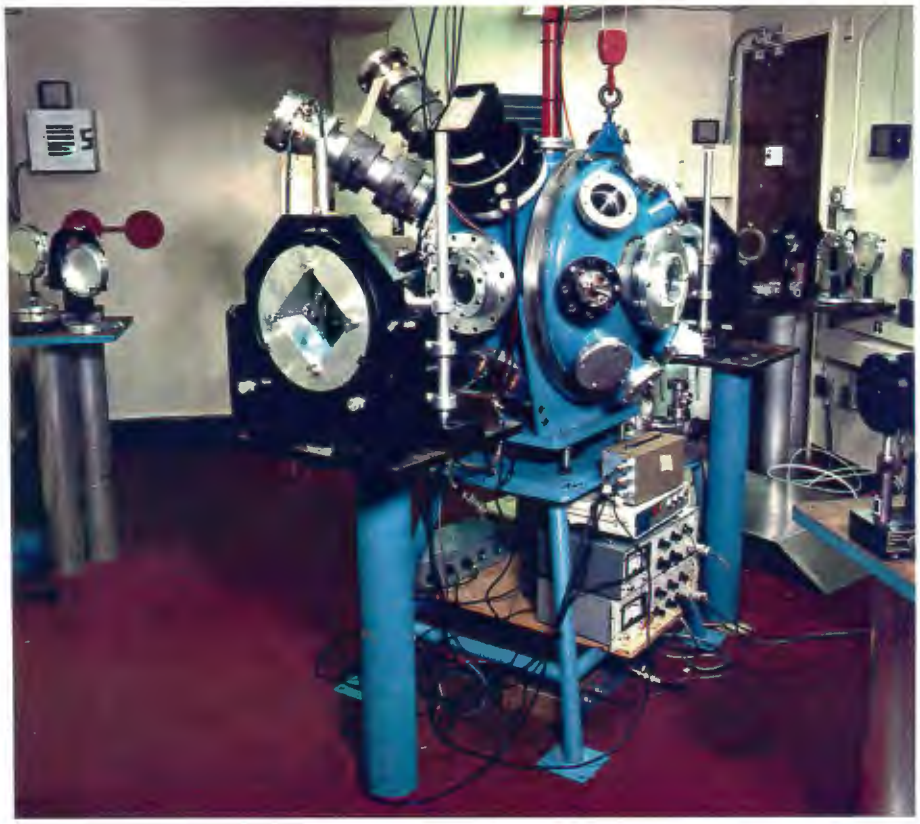

Figure 5. Photograph of the Phoenix laser facility target chamber room B. The door to the chamber (closed) is supported by the red winch at the top of the figure.

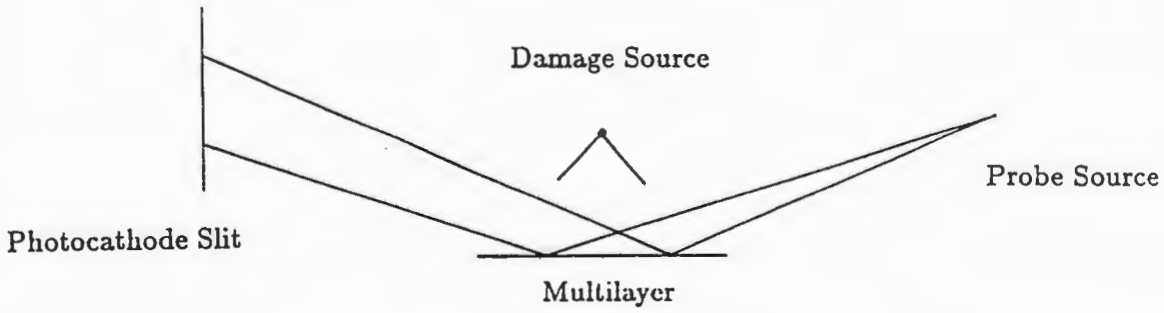

Figure 6. Schematic diagram of the damage experiments. The x-ray sources are laser generated Cu plasmas. The damage source irradiates the multilayer while the probe source provides for reflectivity measurement.

laser shots. First a shot was taken with only the probe beam to verify the alignment of the multilayer. The next shot employed both the probe and the damage sources so that the reflectivity of the multilayer could be monitored during irradiation by the damage source. This was followed by a probe beam shot to verify the damage done to the multilayer.

Two views of the apparatus within the target chamber can be seen in Figure 7. Please note that the quality of the photograph was limited by the LLNL security restriction that only Polaroid cameras can be used by researchers. The multilayer is mounted facing away from the viewer on the aluminum holder at the center of the figure (angled at about 45° clockwise from vertical) with the multilayer in the plane of the figure mounted near the lower end of the holder between the red and blue lines barely visible in the photograph. The holder was constructed to rotate about an axis on the surface of the multilayer parallel to the length of the holder. Translation in and out of the figure as well as rotation about an axis in the plane of the figure 45° counterclockwise from vertical was also provided. The experimental layout was such that one plasma was 2-3 cm from the multilayer along a line normal to the surface of the multilayer to act as a source of damaging x rays with a maximum time-integrated flux of about 250 mJ/cm^2. Due to variations in laser energy, however, the average time-integrated damage flux in these experiments was approximately 150 mJ/cm^2. These damage fluxes were determined from LLNL measurements[20] of x-ray production by Cu plasmas. It was determined that for these laser power ranges approximately 80% of the incident 532 nm light is absorbed by the plasma with 30% of that energy being coupled into Cu L_α x rays for an overall efficiency of about 25%. The damage fluxes quoted were determined by assuming that the x rays are radiated isotropically into the half-sphere above the target. In

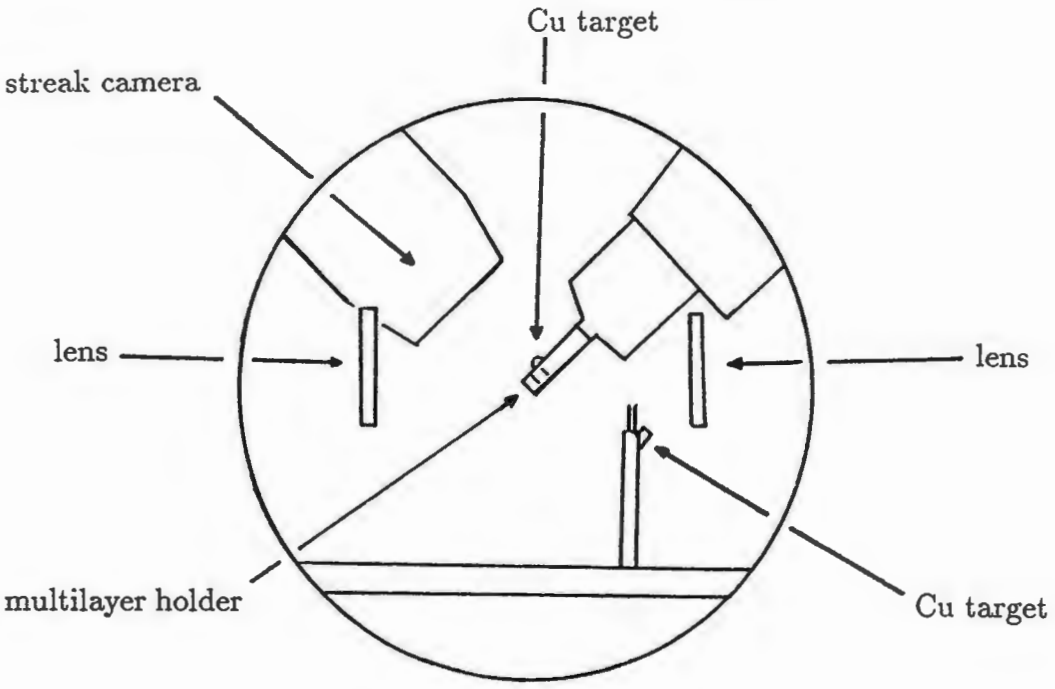

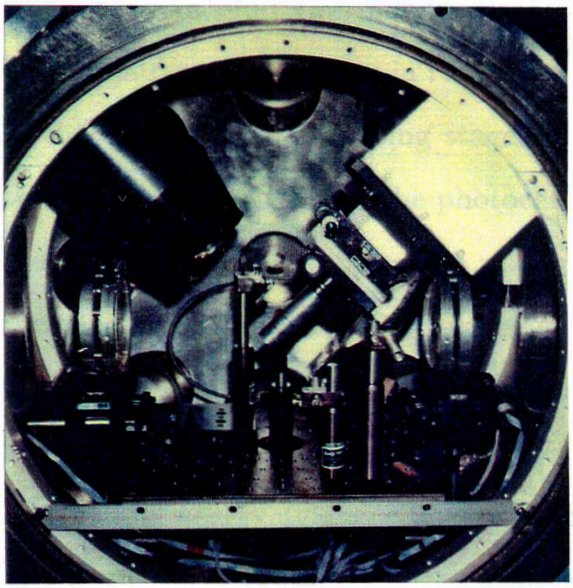

Figure 7. The experimental layout as seen from the door of the target chamber. Fig. 7b is the photograph.

actuality there is a slight maximum in the direction of specular reflection of the laser light. The Cu target used to produce this damage source plasma is barely visible on the left of the multilayer holder in Figures 7a,b. The other plasma generated x rays incident on the multilayer at the Bragg angle (about 18°). This was our probe source. The geometry of the experiment was tailored to the 930-950 eV Cu L_α doublet lines because of the high conversion efficiency (30%) of laser energy into the x-ray lines. The copper target of the probe source is in the lower right hand corner of Figure 7a,b. The laser beam used to produce the probing x rays is focused onto this target by an f/2 lens (right hand side of Figures 7a,b). A 45° angle of incidence mirror is used to redirect the beam onto the target. The position of the probe source target is such that the target and the point of incidence on the multilayer are coplanar with the cathode of the soft x-ray streak camera mounted between 10 and 11 o'clock on the outer edge of the target chamber. The streak camera is visible in figures 5, 7a, and 7b. The position of the probe target was controllable from outside the target chamber via rotating feedthroughs which were linked with cables to the translational mounting stages of the target. Probing x rays reflected from the multilayer then struck the photocathode of the x-ray streak camera which recorded the data on film. Since the risetime of the streak camera was well known temporal synchronization of the camera was provided by the laser trigger pulse mentioned above with the addition of a digitally generated delay. This synchronization was verified during initial tests of the system by firing the probe laser beam at a Cu target and observing the x rays produced with a KAP crystal spectrometer mounted on the streak camera. In addition to the apparatus shown in Fig. 7, a 2 liter LN_2 cold finger was inserted into the chamber to increase the pumping speed so that the shot interval was reduced to the 45 minutes required for cooling of the laser disk amplifiers.

Physical alignment of the multilayer with the probe target and the streak camera was a challenging task. This was accomplished by placing a nylon filament between the focal point of the laser on the probe target (a low power alignment beam was available) and the center of the photocathode slit of the streak camera. This filament was used as a reference to determine the zero translational position of the holder for translation in and out of the plane of Figures 7a,b. The filament also referenced the proper rotational position of the holder for rotation in the plane of the figure. The correct rotational position of the holder about its lengthwise axis and the correct translational distance from the zero established by the filament varied depending on the multilayer used. Given the Bragg angle for the multilayer these variables were determined trigonometrically. Verification of the alignment was accomplished by firing a low power beam at the probe target. With the camera placed in a non-streak mode the Cu L_α doublet x rays generated were reflected from the multilayer and observed as two spots on the film. Because this low power beam used only the smallest amplifier stages of the laser (rod stages) these shots could be repeated every few minutes instead of every 45 minutes as is the case when the high power disk amplifier stages of the laser were used. This greatly facilitated the final alignment of each multilayer.

As was previously described, characterization of each multilayer was a three laser shot process. First a shot was taken with only the probe beam to verify the alignment of the multilayer and to record the reflected intensity vs. time at low flux as a reference. The next shot employed both the probe and the damage sources. This shot measured the reflected intensity vs. time at high flux. This was followed by a probe beam shot to verify the damage done to the multilayer. Subsequent to each shot a calibrated Xenon flashlamp was used to expose the film through a linear

attenuation wedge. The camera image and wedge image film densities were then digitized with a PDS microdensitometer and the known exposure wedge densities were used to convert the camera image densities into exposure values. Although the densitometer was capable of 20 μm resolution a more favorable signal to noise ratio and manageable data file size were achieved by digitizing on a 100 μm by 20 μm grid. Image analysis of the digitized data was accomplished with the program OWOW which was developed at BYU for use in these experiments. OWOW converts the film density data to exposure data and has the capability of extracting portions of an image, compressing and smoothing data, and taking slices of data.

C. Data analysis methods

The film exposure vs. angle vs. time data described above provides damage information in primarily two ways. First, a line-out of exposure vs. time at a particular angle for a damage shot can be compared to a line-out at the same angle for the reference shot. Differences in the relative curve shapes indicate if damage has occurred. If the reflectivity of the multilayer drops the damage shot line-out will fall off more rapidly than the reference shot line-out. This method yields a relative measure of the reflectivity. A better method would employ two streak cameras, one camera measuring reflected flux and the other simultaneously measuring the incident flux. The reflected flux could then be normalized and absolute reflectivity obtained. Unfortunately, the available space within the target chamber was not sufficient for two streak cameras in these experiments. This is easily seen when considering Figure 7b.

A second indication of damage is a shift in angular position of an x-ray

line. As the multilayer heats and expands the d-spacing change will result in a shift in the Bragg angle for a given wavelength.

D. Experimental results

In the experiments described above we measured the response of a WC/C multilayer. Reference and damage shot data for the WC/C multilayer are shown in Figures 8 and 9 respectively. The Cu L_α doublet lines are visible at 17.6° (950 eV) and 18° (930 eV). Please note that each grid line corresponds to approximately 0.04 ns of time or about 0.06° of angle in Figures 8, 9, and 11. Line-outs of the reference shot and damage shot data taken along the 930 eV line are shown in Figure 10. The time integrated damage flux was 160 mJ/cm^2. The curve for the probe shot has been scaled by a factor of three and therefore appears to be wider than the actual probe shot line-out. Scaling of the curves was necessary due to shot to shot variations in laser energy. The fact that the duration of the probe source is longer in the damage shot can also be attributed to shot energy variations. In each damage shot in our experiments the energy of the probe beam was 2 J less than the 10 J to 14 J for the probe shot even though no adjustments were made to the laser. Not only did this result in longer pulses of x rays but changes in the relative intensities in the spectrum were also observed (see Figure 12). Data for the reference shot taken after the damage shot is shown in Figure 11. Note that there is no evidence of the doublet lines and there is little reflected energy. This data indicates that the multilayer has been destroyed.

A similar experimental sequence was repeated using a W/C multilayer. Reference and damage shot data for this multilayer are shown in Figures 13 and 14.

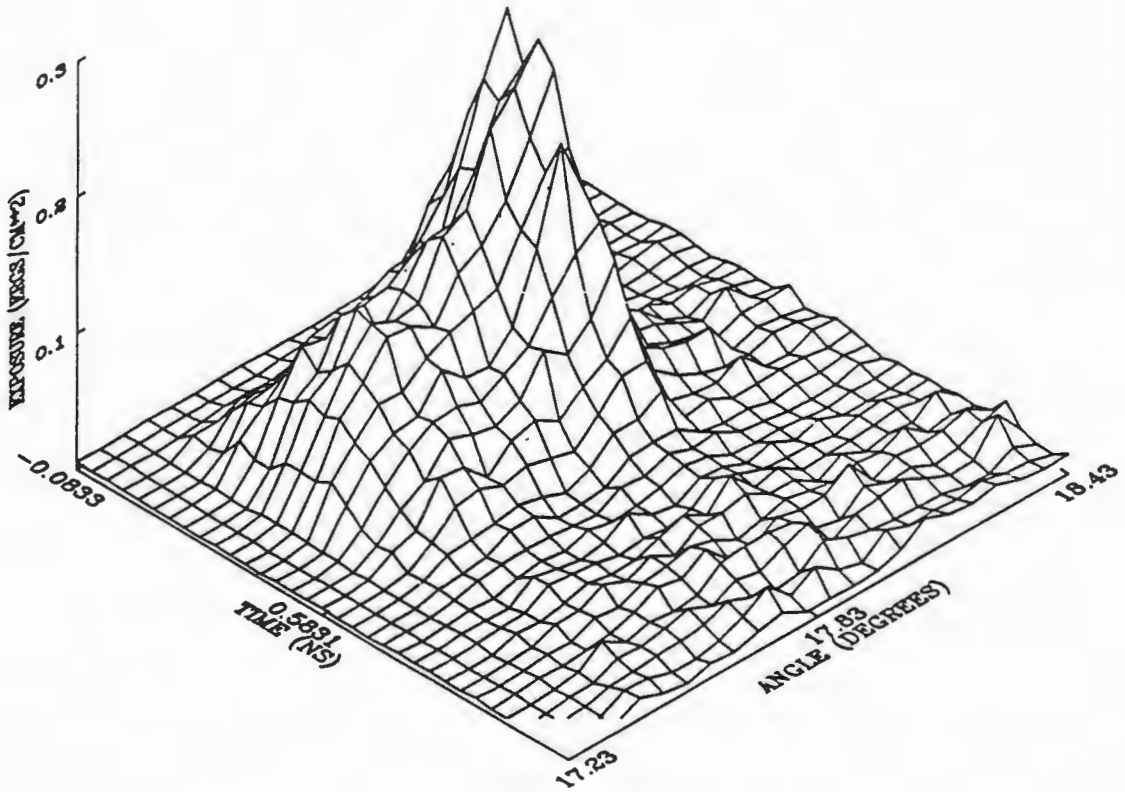

Figure 8. Reference shot data (Shot 89) for the WC/C multilayer.

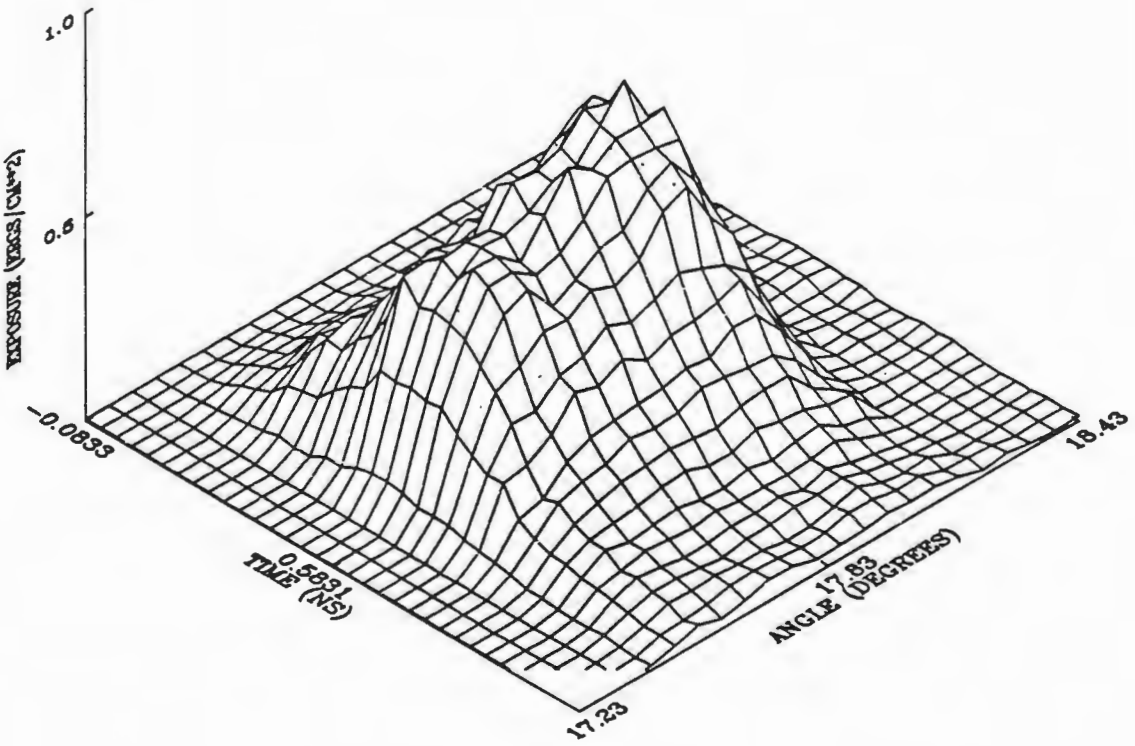

Figure 9. Damage shot data (Shot 90) for the WC/C multilayer.

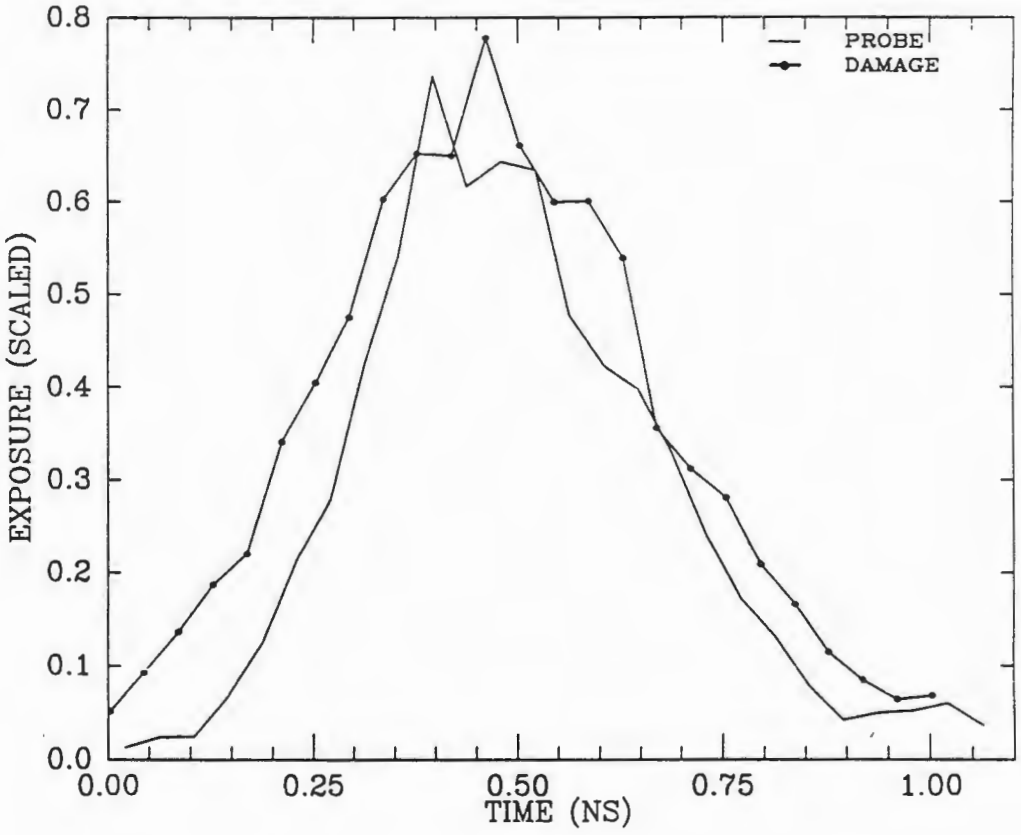

Figure 10. Line-outs of the reference and damage shot data for the WC/C multilayer taken along the 930 eV line. The curves have been scaled to allow for comparison.

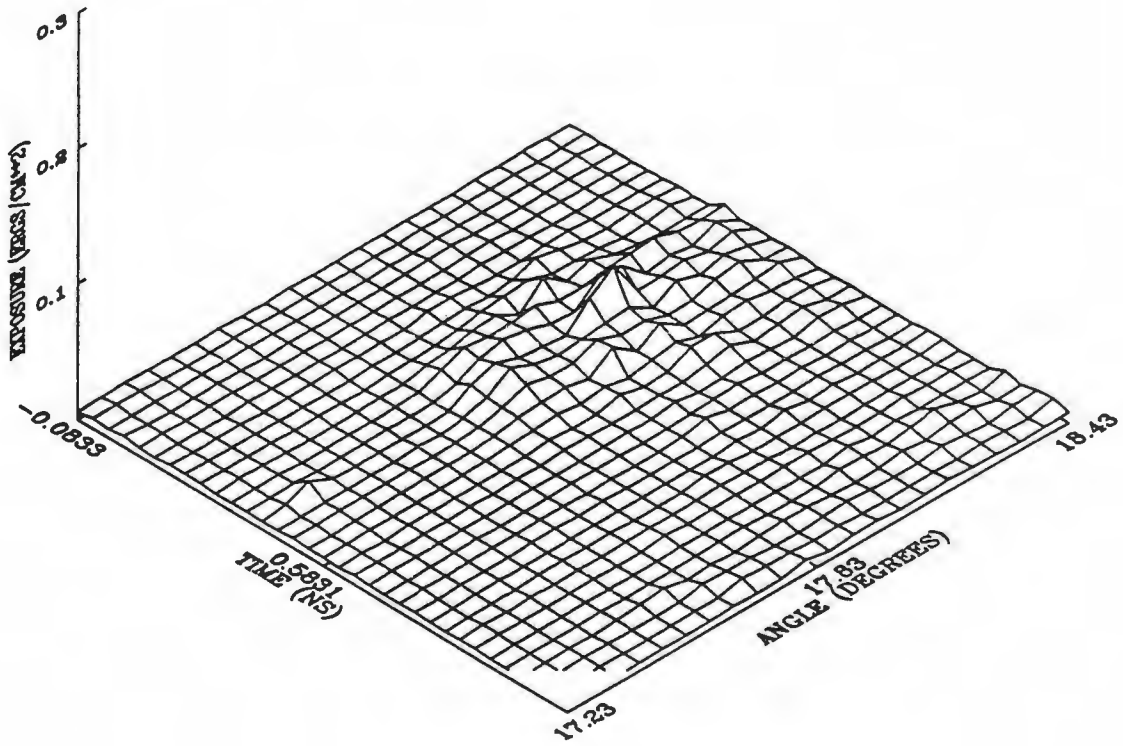

Figure 11. Post damage reference shot data (Shot 91) for the WC/C multilayer. Note that the scale is smaller than in Figure 9.

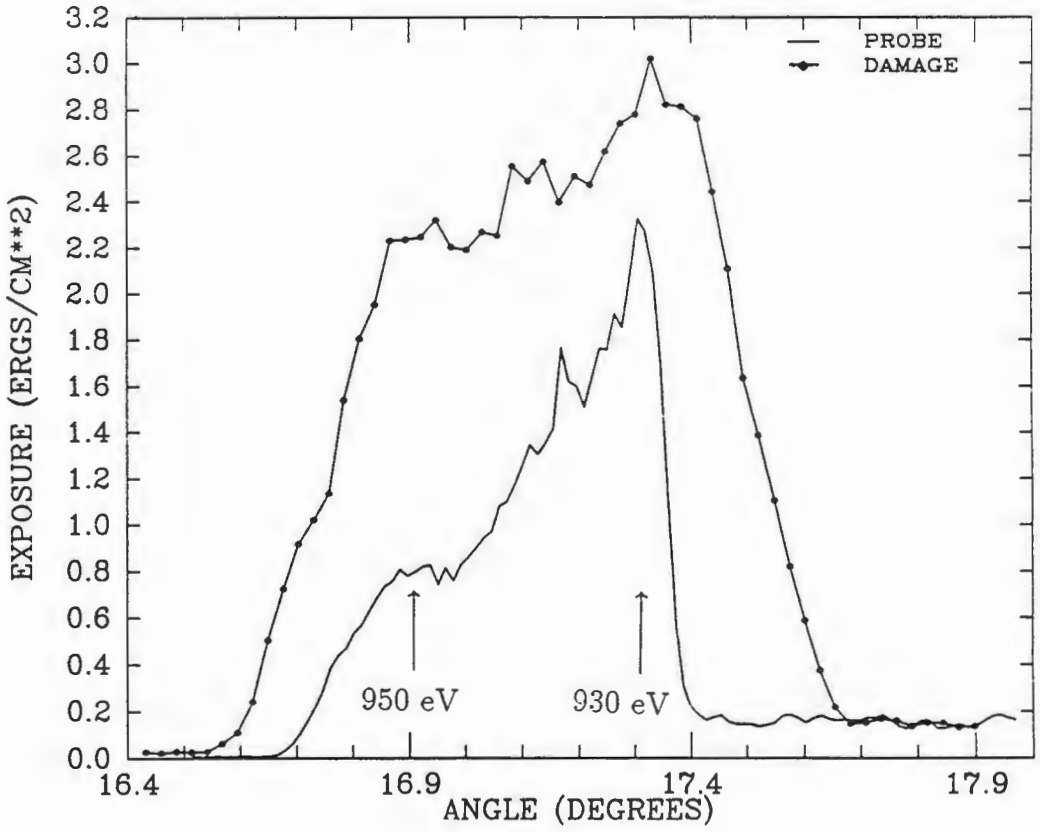

Figure 12. X-ray spectra of the probe beam source at laser energies of 14 J (probe-Shot 104) and 12 J (damage-Shot 105). Note the shift in relative heights of the 930 eV and 950 eV lines.

The time-integrated flux in this damage shot was 120 mJ/cm^2. The resolution of this multilayer is poorer than that of the WC/C, however, and the Cu L_α doublet is not as easily distinguished. The line-outs taken from these plots are presented in Figure 15 and again show no observable damage within the duration of the laser pulse. Data from the reference shot (Figure 16) taken subsequent to the damage shot indicate that this multilayer was also destroyed.

Based on the data shown these multilayers maintained significant reflectivity for at least the duration of the laser pulse but were eventually destroyed. Since the lines do not drop off drastically after peaking it can be inferred that not only do the multilayers maintain some reflectivity but the reflectivity is close to peak reflectivity. This raises the question of when does the reflectance dimish. We considered delaying the probe beam with respect to the damage beam to look for damage at some time after 1 ns but at the time we did not have any estimate of when the damage would occur. An alternative was to increase the flux of damaging x rays either by increasing the laser energy or moving the multilayer closer to the damage source. The latter was not possible due to size of the focal cone of the laser beam (f/2 focusing lens) and the close (2-3 cm) proximity of the Cu target and the multilayer mount. If more energy had been available from the laser the damage would have been more likely to occur during the duration of the probe pulse.

We hoped to see evidence of damage during irradiation by noting shifts in the Bragg angle of the multilayers. This, however, was impossible due to the construction of the streak camera which allowed the film holder to rotate about an axis perpendicular to the film. Thus the orientation of the temporal sweep of the camera with respect to the film edge was not known. If a shift in the position of the

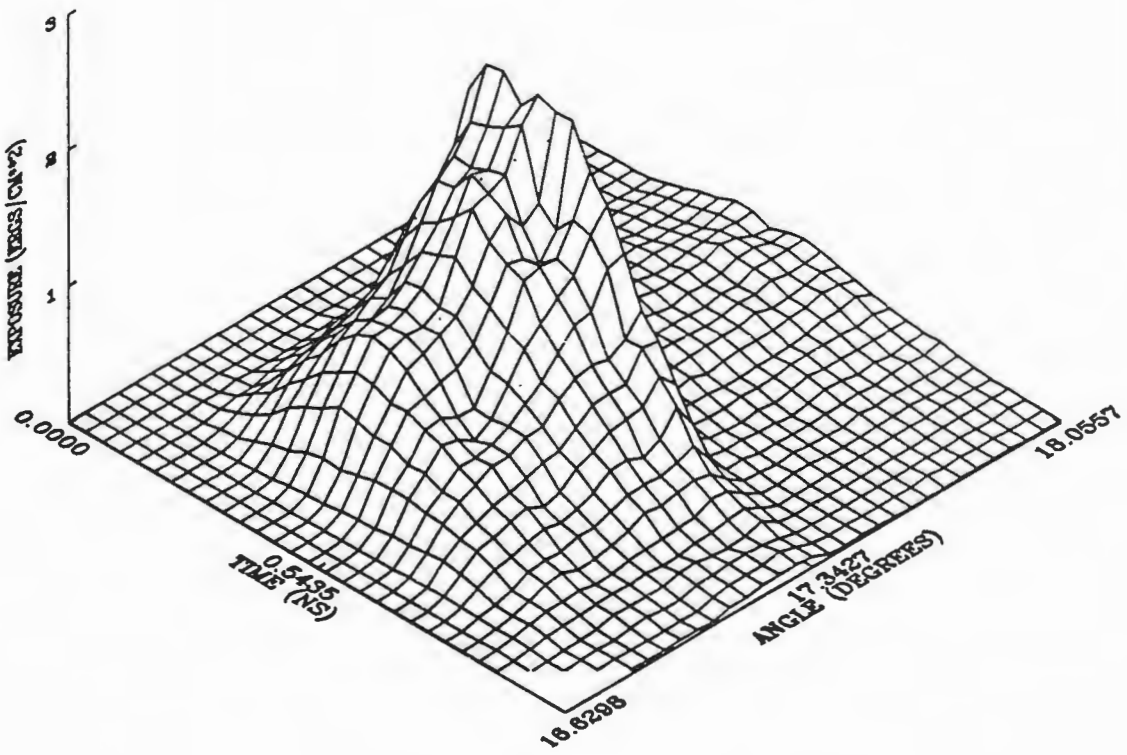

Figure 13. Reference shot data (Shot 104) for the W/C multilayer.

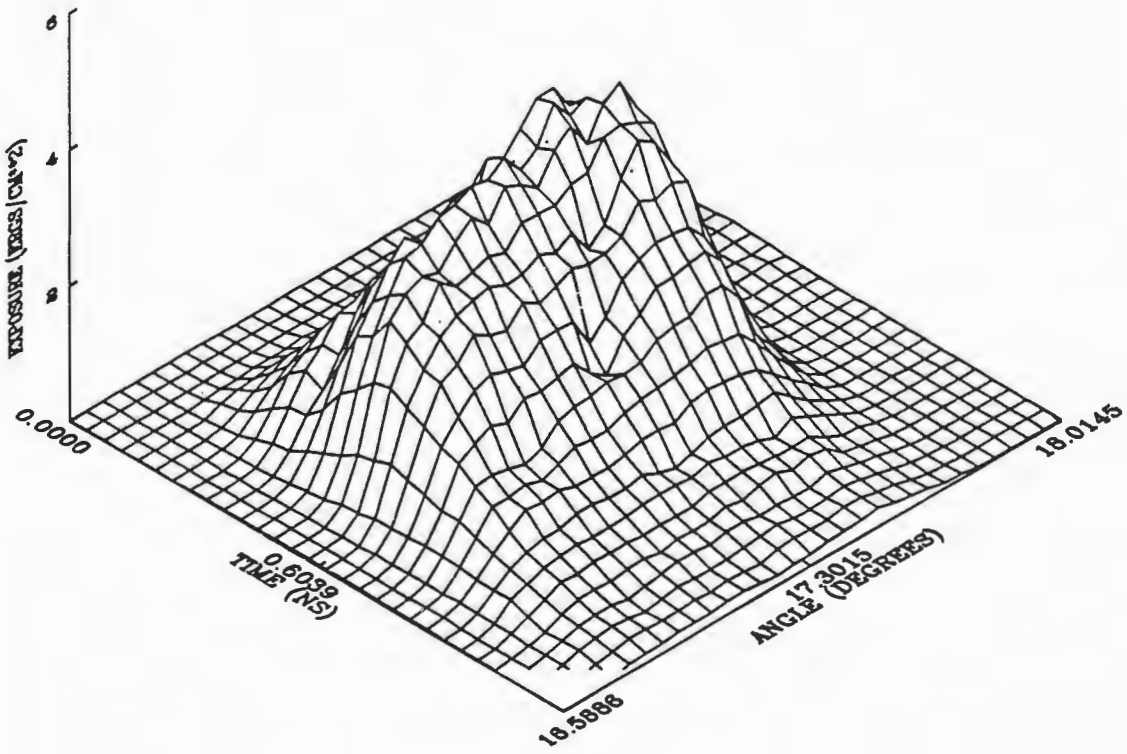

Figure 14. Damage shot data (Shot 105) for the W/C multilayer.

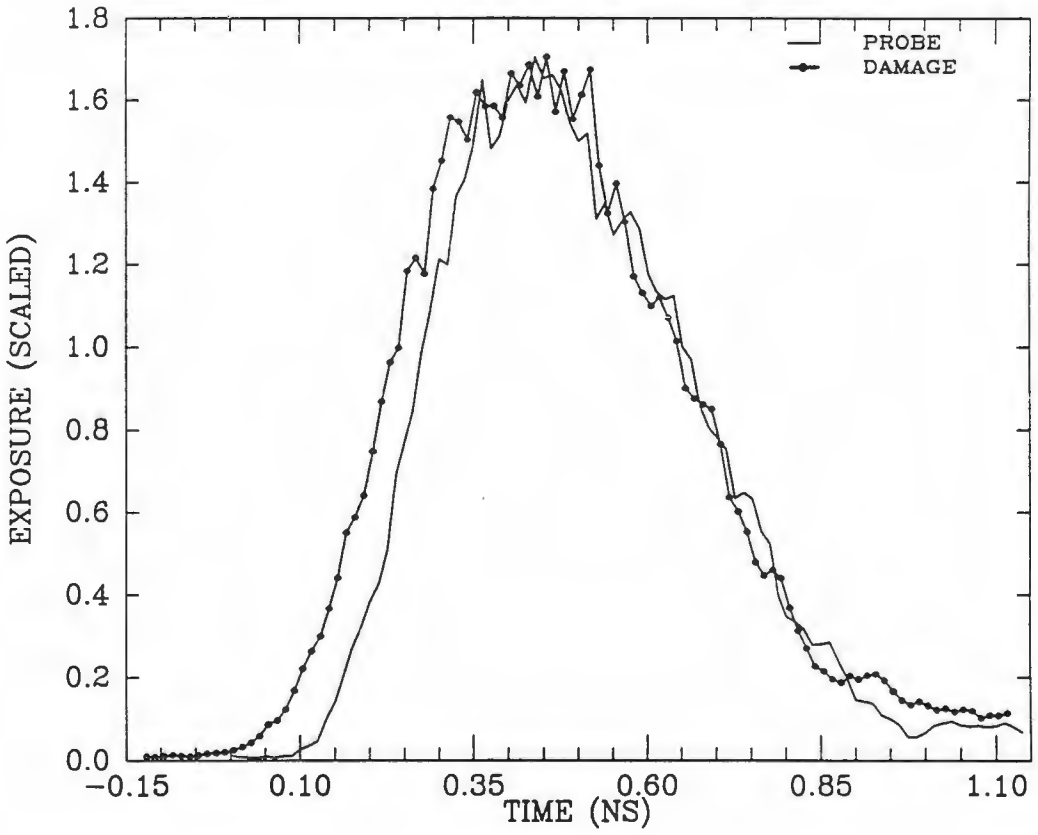

Figure 15. Line-outs of the reference and damage shot data for the W/C multilayer taken along the 930 ev line. The curves have been scaled to allow for comparison.

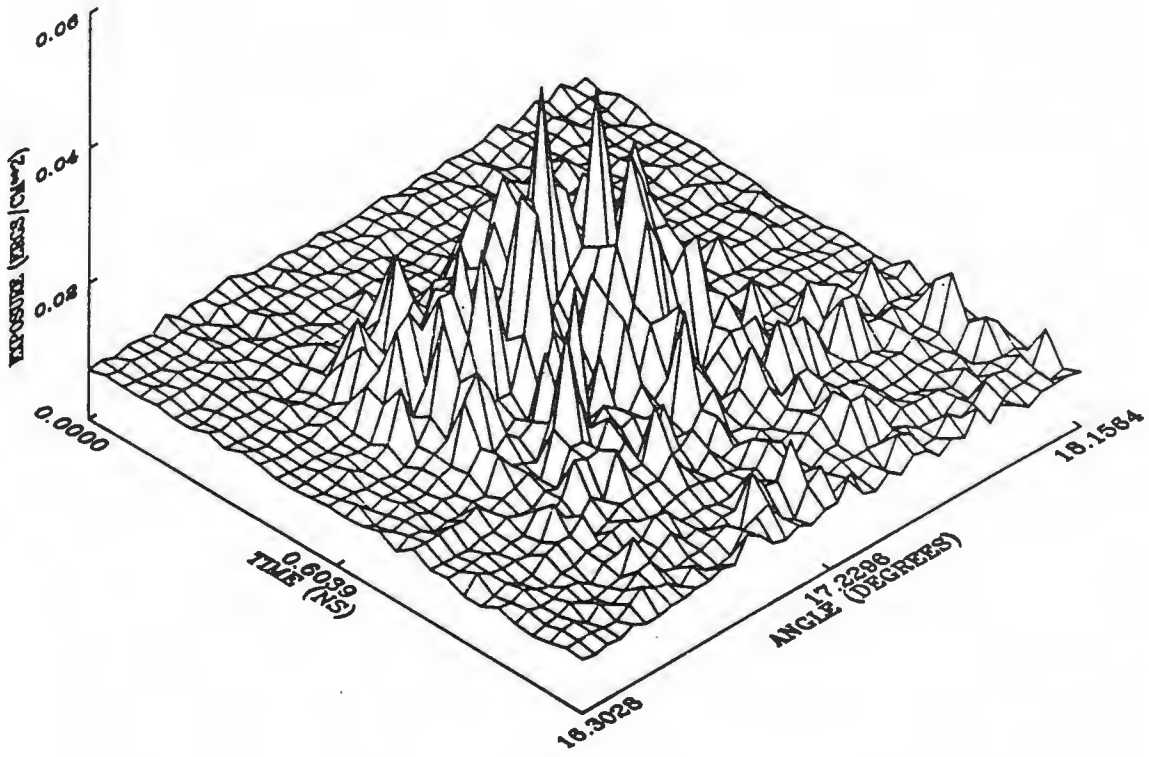

Figure 16. Post damage reference shot data (Shot 106) for the W/C multilayer. Note that the scale is smaller than in Figures 13 and 14.

spectral lines on the film were seen it would be unclear if the shift was due to damage or film rotation. In theory it should also be possible to observe convergence of the lines as the d-spacing increases. This is not possible, however, because an increase in d-spacing of the multilayer by about 10% or approximately 2 Å, as predicted by ROMULS, leads to a decrease in the line spacing of only about 60 μm which is only three pixel widths or a shift of one point on the digitization grid. Considering the noise inherent in film density digitization this effect would be nearly impossible to observe.

Due to the proximity of the damage source to the multilayer the possibility existed that the damage observed was due to plasma blow off from the damage source as opposed to damage from x-ray absorption. This would explain the failure to observe evidence of damage during the irradiation period. In order to measure the relative strength of each mechanism we covered one-half of a WC/C multilayer with a thin (5 μm) Be foil and then irradiated it. Both halves of the multilayer appeared dull and hazy but the unshielded side showed small blotches due to copper condensation on the multilayer surface. The condensed copper spots were sufficiently dense on some areas of the multilayer to destroy its visible reflectivity. A similar procedure was repeated using a Ti/C multilayer. Subsequent to irradiation the two Ti/C multilayer samples were evaluated via Cu K_α x-ray diffraction. X-ray diffraction data for the covered and uncovered Ti/C samples is given in Figure 17. Prior to irradiation the Ti/C multilayer *d*-spacing was 30.0 Å with a reflectivity of about 40%. The upper diffractometer trace in Figure 17 shows that the multilayer covered by the 5 μm Be foil has sustained significant damage. The vertical scale is such that the maximum reflectivity is 0.03%. Note that two peaks appear, indicating loss of coherence in the layer thicknesses. The *d*-spacings determined from

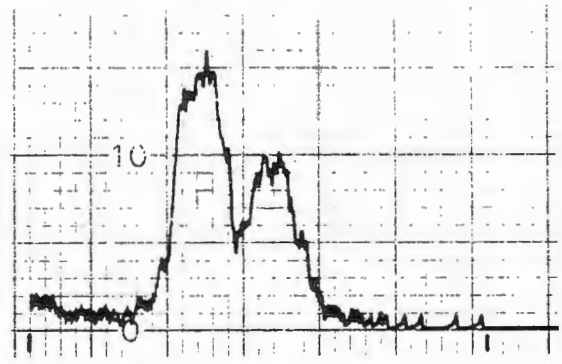

2.0° 3.5°

2.0° 3.5°

Figure 17. X-ray diffraction data for Ti/C multilayer samples after irradiation. The upper trace corresponds to a sample covered by a 5 μm Be foil. The lower trace corresponds to an uncovered sample. The vertical scale is equal on both traces and represents a reflectivity drop of a factor of 10,000.

the angles of the peaks are 35.0 Å for the larger peak and 32.0 Å for the smaller peak. The lower diffractometer trace corresponds to the uncovered Ti/C multilayer sample. The vertical scale is the same as in the upper trace, indicating an additional loss of reflectivity of about a factor of two from the covered sample. Only one peak is seen, at an angle corresponding to a d-spacing of 36.5 Å. This does not necessarily imply that the layers have regained coherence; it is likely that a few of the inner layers have expanded similarly while the outer layers have sustained such damage that all reflectivity is lost. This will be further discussed in the next section (section III.E.). The fact that both the covered and uncovered multilayer samples show reflectivity losses of four orders of magnitude demonstrates that for the plasma conditions in these experiments the multilayers were damaged by irradiation and not by plasma bombardment. This result also implies that x-ray irradiation provides the energy which damages the multilayer but the damage mechanisms act over time scales longer than the period of irradiation.

E. TEM analysis of damaged multilayers

As a further study of damage mechanisms we obtained TEM (Transmission Electron Microscopy) micrographs of WC/C and W/C multilayers taken before and after damage. The micrographs for the WC/C multilayer before and after damage are seen in Figures 18 and 19 respectively. Before damage the multilayer has a uniform structure and little roughness. After damage the structure is good only near the substrate overcoat (thick white band at the bottom of Figure 19). Also, note that the damage appears progressively greater towards the surface of the multilayer. This is corroborated by the ROMULS prediction and intuitive expectation that the maximum temperature reached in each layer decreases with depth. Com-

parison of the before- and after-damage micrographs for the W/C multilayer shown in Figures 20 and 21 shows the microscopic changes in the multilayer. No layer structure is visible and there is obviously significant surface damage. Despite the lower magnification in the micrograph it is clear that the WC/C multilayer is more robust than the W/C even for greater x-ray fluxes, although both are eventually destroyed.

Although the micrographs show the details of the multilayer structure they give no indication of the material phases which result from irradiation. For example, it is desirable to know if WC or W_2C forms as a result of irradiation of a W/C multilayer. It might be possible to obtain this information from electron diffraction patterns if crystallization ocurrs in the sample. Auger electron spectroscopy could also provide phase information.

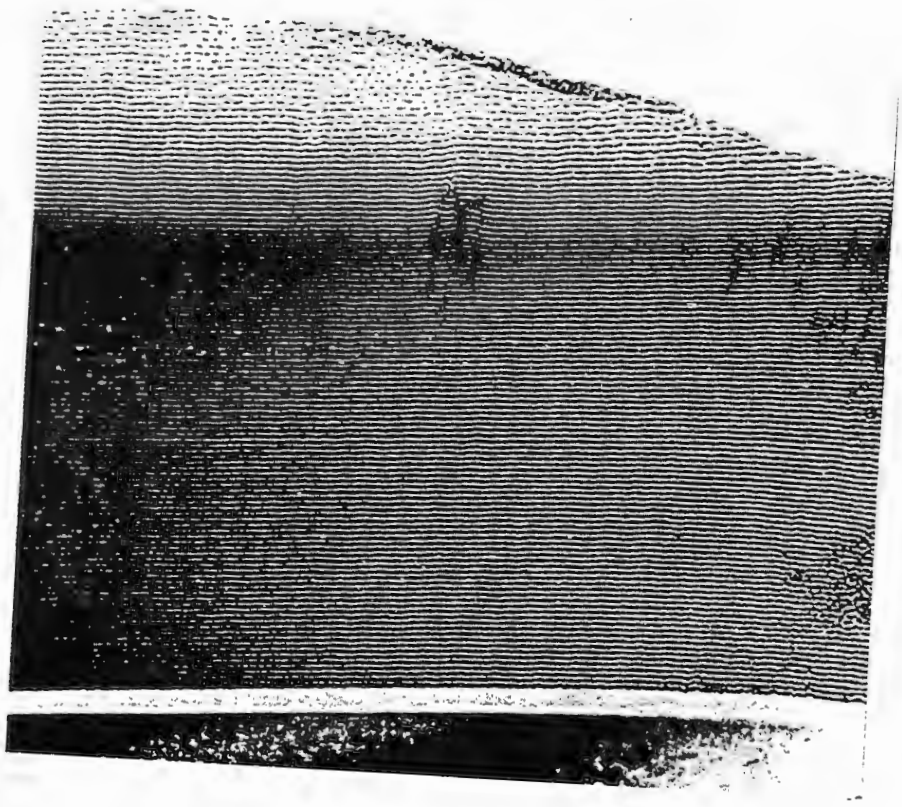

Figure 18. Micrograph of the WC/C multilayer (magnification 355,000 X) before irradiation. The damage at the top of the multilayer is a result of sample preparation. The white band at the bottom of the figure is a carbon undercoating.

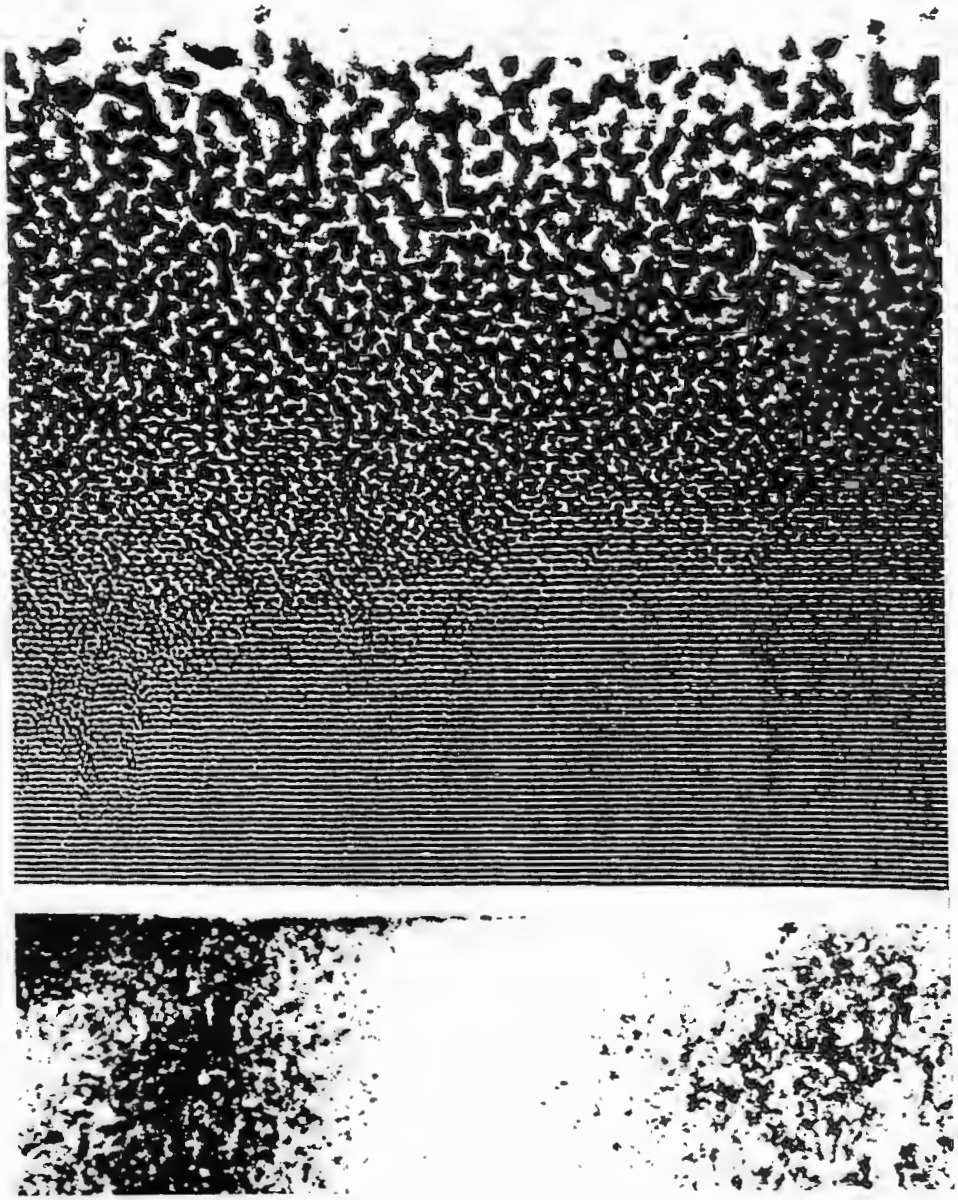

Figure 19. Micrograph of the WC/C multilayer (magnification 355,000 X) after irradiation. Note the progressive loss of structure towards the top of the multilayer.

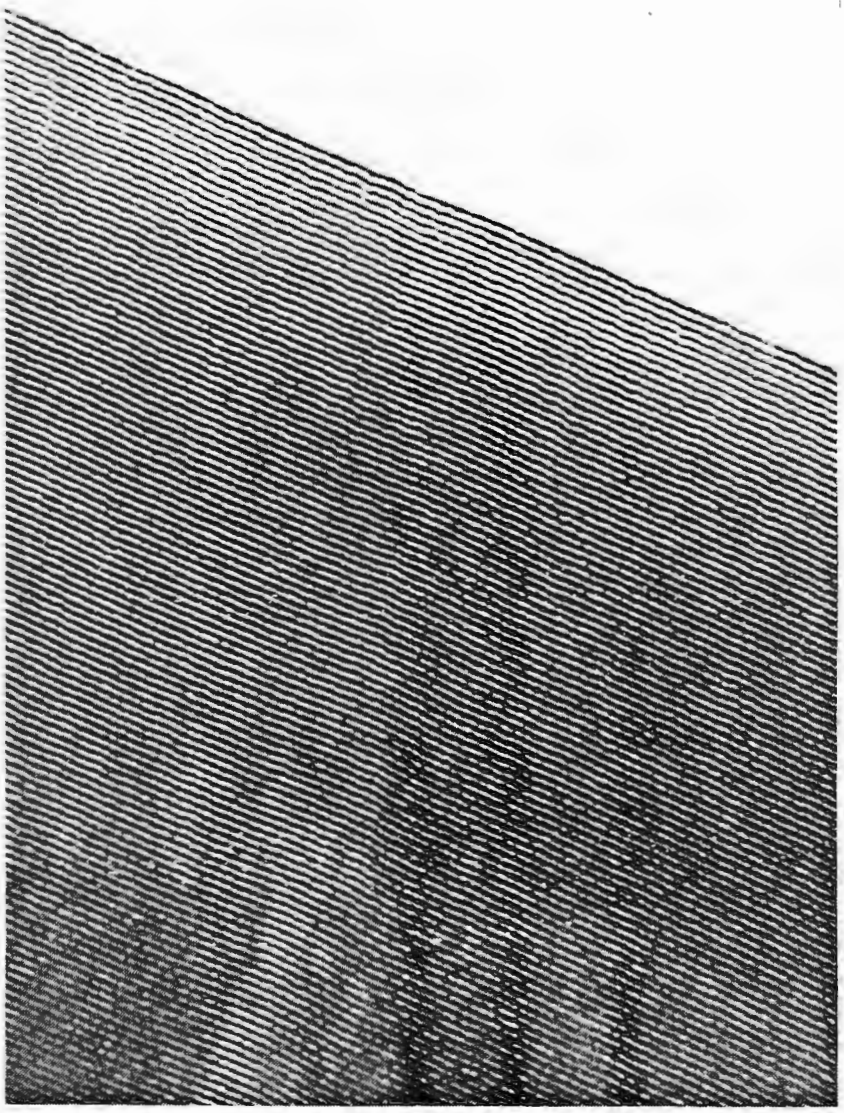

Figure 20. Micrograph of the W/C multilayer before damage. Because of the high magnification (504,000 X) not all of structure is visible but other micrographs show equal multilayer quality.

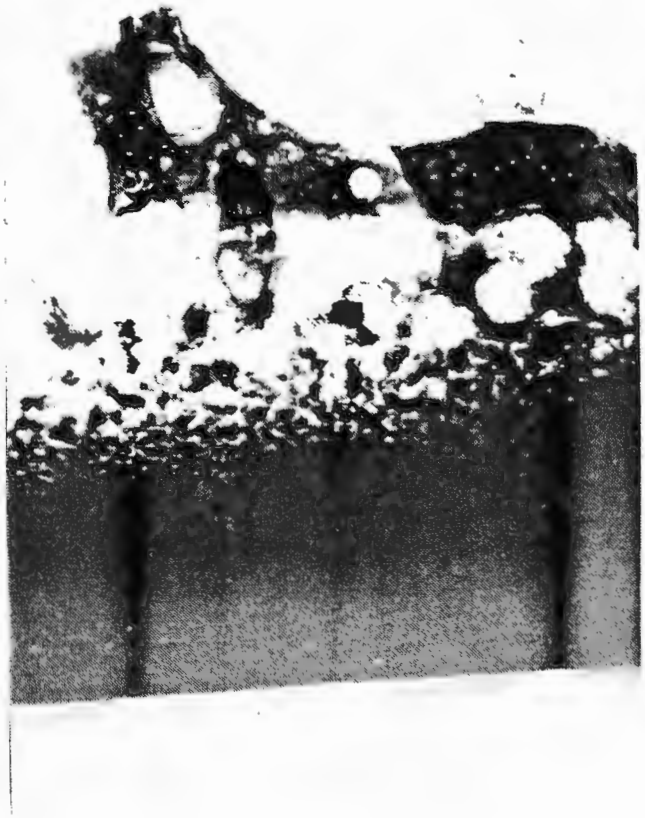

Figure 21. Micrograph of the W/C multilayer after damage. Because of the severe damage to the film only lower magnification (168,000 X) imaging was possible. There is some evidence that the damaged structure is similar to that seen in Figure 19.

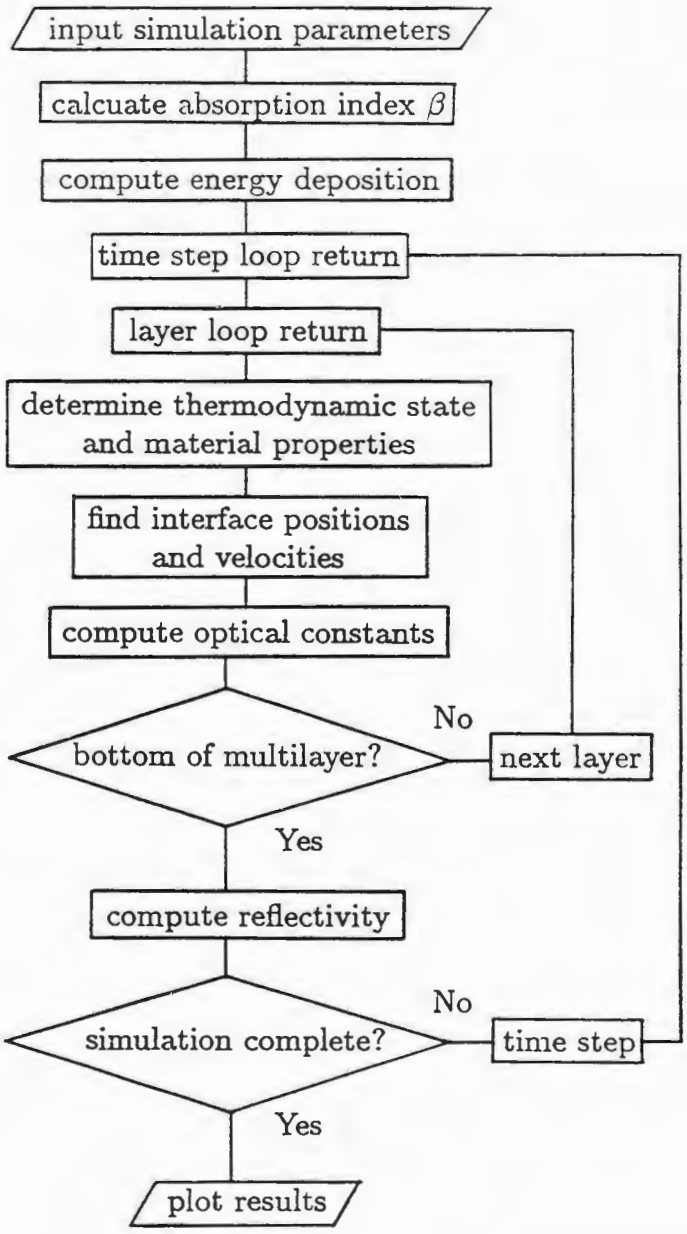

Figure 22. Flow chart of the RObust MULtilayer Simulation code ROMULS.

IV. COMPUTER MODELING OF DAMAGE

Because of the difficulties and complexities involved in experimental characterization of multilayer response in high flux applications it is desirable to model and predict this response. If a model were available which made reasonable predictions of actual observations it would be a valuable tool in the design of robust multilayers. Furthermore, optimization of such a model would give insight into the damage mechanisms important in these applications.

A. Previous modeling efforts

Prior to this work several groups reported efforts to model the response of multilayers to fluxes of x rays sufficient to heat and damage the mirror. Computational attempts to estimate the absorbed energy required to melt multilayers were reported by More[21] and Kania[22]. These models lacked, however, any means of assessing damage prior to melting. Hockaday[17] developed a computational method for predicting the reflectivity versus time of multilayers in the experiments described in reference 17. The code, however, underestimated the useful life of multilayers by a factor of 82.

B. The ROMULS simulation code

A code to predict the response of a multilayer to damaging fluxes involves the following three computations. First, the energy deposited in the multilayer by x-ray absorption is calculated. Then the effect of the absorbed energy on the multilayer can be determined. This involves both changes in the thermodynamic

state of the materials and the physical state and size of the layers. Finally, once the new structure and state of the multilayer is known the reflectivity can be computed. Ideally these three steps would be repeated over many small time increments to yield the simulated multilayer response for the total time.

The code ROMULS is a driver and user interface for other codes which perform the computational functions indicated above. A flow chart for ROMULS is presented in Figure 22. above. In our code the absorption of x rays by the multilayer is calculated by XRAYCARP, a routine developed at Brigham Young University (BYU). The model employed in this code is exponential absorption, which is a good model for thin structures such as multilayers where deposition due to reradiation is not significant. For simplicity the incident radiation is assumed to be monochromatic. The consequences of a multicomponent spectrum are discussed below.

The ratio T of transmitted intensity to incident intensity is given by

$$T = \frac{I_T}{I_0} = e^{-\mu\rho x} \tag{3}$$

where μ is the mass absorption coefficient, ρ is the density, and x is the material thickness. The mass absorption coefficient is given by

$$\mu = \frac{2r_0\lambda N_A}{A} f_2 \tag{4}$$

where r_0 is the classical electron radius, N_A is Avagadro's number, A is the atomic mass, and f_2 is an experimentally determined atomic scattering factor. In the complex index of refraction, $n = 1 - \delta - i\beta$, β is known as the absorption index and is related to the scattering factor f_2 by

$$\beta = \frac{r_0\lambda^2 N_A\rho}{2\pi A} f_2. \tag{5}$$

Combining equations (4) and (5), equation (3) becomes

$$T = e^{-4\pi\beta x/\lambda}, \tag{6}$$

the form used in XRAYCARP. On-line versions of Henke's f_2 data tables[23] are used with standard bulk densities to compute T for each multilayer material. Multilayers often consist, however, of materials which as deposited are amorphous. In general for common multilayer materials the densities of the amorphous layers are less than the densities of the bulk materials. The exact values depend on deposition conditions and hence are not well known. This density error could lead to a significant overestimation of absorption. As an example, if we assume $\rho = 0.8\rho_{\text{bulk}}$ for either of the W/C multilayer simulations described below the absorption coefficient for each layer decreases from 0.0235 to 0.0188, a 20% decrease.

The absorption coefficient A is the ratio of absorbed intensity to incident intensity. In most cases we know that the absorption calculated by the code is too great because XRAYCARP assumes that energy not transmitted is absorbed when in reality some of that energy is reflected by the multilayer. In terms of the reflection, absorption, and transmission coefficients the code assumes $A = 1 - T$ when in fact $A = 1 - T - R$. For most multilayers the reflectivity is at least 10% and is often much higher. Correction of this error would require that the absorption code be capable of computing reflectivity. The absorption error is also important if the spectrum is not monochromatic. In such cases the flux of x rays at wavelengths other than the wavelength of the simulation should be included in the total flux input to the code. For a spectrum with major components which are not reflected the absorption predicted by the code will be the same as for the monochromatic case where it is assumed that $R = 0$. Alternatively, if the spectrum has a major component near the resonance of the multilayer the predicted absorption will be

high. This is often the case since a multilayer would most likely not be used if it had poor reflectivity at the desired wavelength.

Since the total mass in each layer is conserved, T is a constant [The product βx is a constant. See equations (5) and (6)]. The intensity at any depth in the multilayer can therefore be integrated over time to obtain the total energy transmitted or absorbed at that point. Given the time-integrated flux E_0 (total energy) incident on the surface of the multilayer the energy absorbed by the first layer is AE_0 and the energy transmitted to the second layer is TE_0. By iteration the energy absorbed by each layer during the course of the simulation can be found. This energy is then input into the material response code.

To gauge the damage done to the multilayer materials and structure we have employed the material response code CHARTD, a one-dimensional radiation-hydrodynamic code developed at Sandia Laboratories.[24] The basic operation of the code is given in reference 24. Briefly, for a series of small time steps CHARTD takes the energy absorbed in each layer and determines the new thermodynamic state of the layer based on its numerical equation of state. The position and velocity of the layer boundaries are then determined by conserving mass, energy, and momentum. We have made several modifications to the code. First, to allow for more materials so that multilayers can be treated. Also, the code now periodically writes a layer structure file containing the interface positions and material densities for later use in reflectivity calculations. Since the code had previously been used only on Cray and CDC systems we modified the code to run under VAX VMS. This included converting the numerical equation of state routines to run in double precision.

The material response code CHARTD is a one-dimensional code which assumes uniform material layers, hence there are several damage mechanisms which are unaccounted for. For example nonuniformities in the heating of the layers could lead to roughness of the interfaces. Also, the possible diffusion of atoms across the material interfaces is not modelled. Another unaccounted effect which has been observed is crystallization of amorphous layers. None of these omissions, however, are likely to affect the accuracy of the simulations. The overall changes in the layers are so great that nonuniformities in heating will be a second order effect. Diffusion is not an important damage mechanism because for most applications materials can be chosen which have virtually no mutual solubility. Even for material pairs which are somewhat soluble diffusion is not the observed damage mechanism (see references 10 and 11). Crystallization of amorphous layers has been observed by Ziegler[11] in isothermal annealing experiments on time scales of hours but no observations of crystallization in pulsed x-ray applications have been reported.

Two additional cautions apply to material response codes. First, codes such as CHARTD attempt to model complex phenomena and some of the models in the code may lead to erroneous predictions. An example is the analytical equation of state determined by CHARTD. To model the equation of state of a material over the wide parameter region treated by CHARTD from first principles is a very difficult task. Error may also be caused by the material "constants" used to compute the equation of state and other physical properties. In addition to density, other thin-film properties are known to vary greatly from the bulk material properties. For example, the hardness of many thin films is several times the strength of a bulk sample but again exact measurements have been made for only a few materials[25] and the values are dependent on the deposition conditions. The tensile strength of

thin films is also greater than the strength of the bulk materials. Also, the material constants available in the literature are in general taken at room temperature and may be quite different at the high temperatures under consideration. For the materials we have examined the computed equation of state agrees well with available data but this may not be the case for other materials. Furthermore, this code solves the relevant partial differential equations by the finite element method. When applied to problems where the elements are only a few atoms thick, as in a multilayer, the assumption that the elements are continuous is no longer valid but appears, *a posteriori* , to be reasonable.

Similarly, a modeling error results because the version of CHARTD employed in ROMULS does not correctly handle the energy absorbed by the multilayer. The code assumes that the opacity of the materials is constant when in reality the opacity decreases as the temperature increases, especially as the melt transition is approached. While the product of the opacity and the thickness of a layer is in reality constant, CHARTD computes layer thicknesses without correcting the opacity. Thus the layers expand without a concurrent decrease in opacity. This assumption results in an overestimation of the damage caused by the energy.

Once the structure of the irradiated multilayer has been determined the reflectivity is calculated by LSMLAYERS, a program developed at BYU based on the method and code of Underwood,[26] which has proven to be accurate to within a few percent. As mentioned above the input for this code is the positions of the layer interfaces and the density of each of the layers. LSMLAYERS calculates the reflectivity in the following way. Let the subscript j denote the j^{th} layer in the

multilayer structure. We define

$$g_j = (n_j^2 - \cos^2\theta)^{1/2} \tag{7}$$

and for the j^{th} and $(j+1)^{\text{th}}$ layers

$$\Re_{j,j+1} = a_j(E_j^R/E_j) \tag{8}$$

where $E_j^R/E_j = F_j$ is the familiar Fresnel amplitude reflection coefficient,

$$a_j = e^{-i\pi g_j d_j/\lambda} \tag{9}$$

is the amplitude factor at half the distance into the layer of thickness d_j, n_j is the index of refraction of the j^{th} layer, and θ is the angle of incidence measured from the surface. At the interface between the substrate and the first material layer it is assumed that $\Re = 0$. Then using the formula

$$\Re_{j,j+1} = a_j^4 \left(\frac{\Re_{j+1,j+2} + F_j}{\Re_{j+1,j+2} F_j + 1} \right) \tag{10}$$

$\Re$ at each of the interfaces is recursively calculated until $\Re_{12}$, the value at the vacuum-multilayer interface is found. The reflectivity of the multilayer at the specified angle is then given by

$$R(\theta) = \frac{I(\theta)}{I_0} = (\Re_{12})^2. \tag{11}$$

This computation is repeated over the desired angle range for each of the specified time steps. At this point the simulation is complete and the predicted reflectivity vs. angle vs. time can be plotted.

Graphics support for ROMULS is provided by ANALYZE[27], which takes the reflectivity data for each of the time steps and compiles it into a hidden surface or

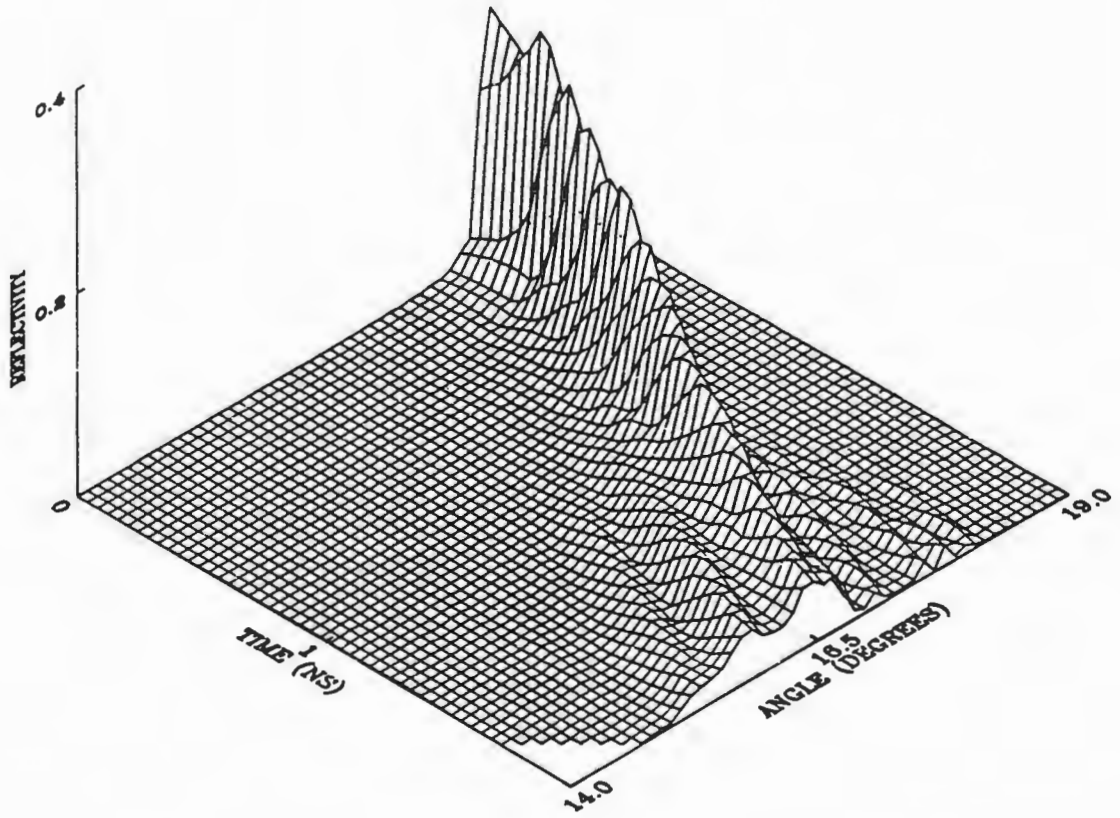

Figure 23. ROMULS simulation of the reflectivity versus angle versus time for the WC/C multilayer used in the Phoenix experiments. (Shots 89-91–see also Figures 8-11).

contour plot of the reflectivity vs. angle vs. time for the simulation. An example of the output of ROMULS can be seen in Figure 23. The plot is reflectivity of the multilayer on the vertical scale versus time and angle. Damage to the multilayer is evidenced by three effects. The first, loss of peak reflectivity over time, is seen by comparing the maximum reflectivity at any time with the maximum reflectivity at some later time. Second, the shift in the Bragg angle with time, indicates that the layers are expanding as temperatures in the multilayer increase. Finally, the appearance of subsidiary peaks is a result of loss of uniformity in the layer thicknesses of the multilayer. Multiple d-spacings in the multilayer allow for multilple reflection peaks. Several features in the plot should be noted to aid in interpreting the data. While it would be expected that the reflectivity would vary smoothly over the course of the simulation it will be noted in Figure 23 that the reflectivity appears to rise and fall in humps. The humps in the data are due to the size of the interpolation grid. Note that each hump corresponds to the data along a line of constant angle. Since the angle of peak reflectivity is rapidly shifting the time-angle interpolation grid cannot linearly connect the two successive points and the hump appears. The plot could be smoothed by a more dense interpolation grid but the readability would suffer.

Care must be taken when interpreting the time of destruction of the multilayer from the reflectivity plots. In most cases the reflectivity of the multilayer drops severely before any of the layers begin to melt (or vaporize in the case of carbon) but in some of our simulations multilayers have shown reflectivity after a significant number of layers have melted. For this reason it is necessary to examine material phase data from CHARTD.

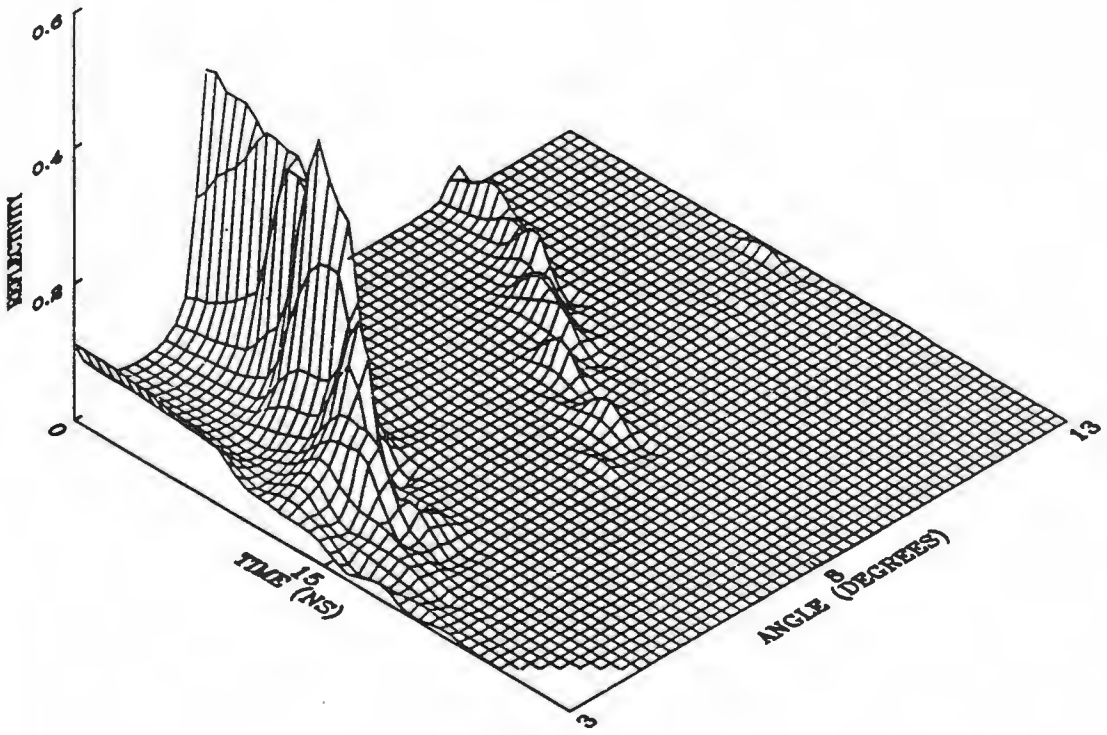

Figure 24. Simulated response of a W/C multilayer to a fluence of 15 J/cm^2 in 70 ns (average power 215 MW/cm^2). The shift in the Bragg angle of the first and second order peaks corresponds to a d-spacing increase from 67.5 Å to about 85 Å. The experiments simulated were performed by Hockaday *et al.*[17]

C. Comparison of simulations and experiments

As mentioned above if one is relying on simulations to design multilayers it is vital to know how the predictions of the code compare with experiment. The data shown in Figure 24 is a simulation of experiments at Los Alamos National Laboratory[17] where a tungsten/carbon multilayer (d =67.5Å) was exposed to an time-integrated flux of 15 J/cm^2 in 70 ns at a wavelength of 12.1 Å from a Z-pinch plasma source. Hockaday observed a drastic drop in the reflectivity of the multilayer after 28 ns.[18] Note in Figure 24 that the reflectivity decreases sharply at approximately 11 ns. This comparison indicates that the code underestimates the life of the multilayer by about a factor of two and a half. In another shot,[19] Hockaday observed degradation of a similar tungsten/carbon multilayer in 19 ns, after exposure to 2 J/cm^2. ROMULS predicted a sharp drop in reflectivity at 10 ns in this case. The drop in reflectivity of the multilayer in both simulations is concurrent with the melting of some of the layers. Note that an error of a factor of two to three represents a substantial improvement over previously reported results as described in Section IV.A.

Experiments we have performed (described in Section III) also indicate that the code underestimates the life of multilayers. The simulated response of the WC/C multilayer used in our experiments is shown in Figure 23. The incident radiation is assumed to be monochromatic with a wavelength of 13.33 Å. The time integrated flux in the simulation (160 mJ/cm^2) corresponds to the value in the actual damage shot. Initially the reflectivity of the multilayer is 25%. After 1 ns the multilayer reflectivity has decreased to 15% with a slight shift in Bragg angle. Peak reflectivity after 2 ns is 4% but the appearance of substantial subsidiary reflection

peaks indicates that the multilayer has been severely damaged. Although we could not obtain data to validate the prediction of destruction at 2 ns it was observed that the multilayers lasted at least 1 ns. Based on comparisons of the predictions of ROMULS with results of the other experiments described the multilayer probably maintained reflectivity for about 4 ns.

To place these results in perspective it is necessary to understand the uncertainties in the experiments. In our experiments and the experiments reported by Hockaday the reflectivities reported are relative and therefore uncertain. Changes in reflectivity, however, are more informative than the absolute reflectivity because they indicate damage and therefore relative measurements will suffice. Also, it is difficult to make absolute measurements of the fluxes involved so that the damage fluences quoted above may be in error. Since these fluences are the basis for the simulations reported this represents a large uncertainty.

V. SUGGESTED IMPROVEMENTS AND FUTURE WORK

Although widespread interest in robust multilayers has waned since this work was completed it is likely that the problem of high-flux damage to multilayers will resurface. Since most of the interest in multilayer damage coincided with the first x-ray laser experiments and it was determined at that time that common multilayers will generally last longer than the lifetime of the laser gain medium most researchers are content with the current technology. Many schemes have been proposed, however, to build laboratory scale x-ray lasers[28,29,30] and in some cases much longer gain medium duration could be expected. As cavities are engineered for these lasers the selection of multilayers may be critical to maximize laser output. With that view toward the future I make the following suggestions for improvement in this work.

A. Improvements in simulations

The operation of computer code ROMULS is depicted in the flow chart in Figure 22. As was discussed earlier the code errs in that it calculates the energy deposition in the multilayer prior to evaluating the damage to the structure. The accuracy of the code could be improved by computing the deposition for each time step using the materials constants for the last time step. This could probably be accomplished by the LSMLAYERS routine which calculates reflectivity since it calculates the fields in each layer anyway. A modification would be required to CHARTD to allow it to read the deposition from a file instead of from its initial input so that the deposition could be determined during the course of the simulation. This would also provide a solution to the problem of calculating the absorption as $A = 1 - T$ instead of $A = 1 - T - R$. Further improvements in the simulations

could be realized by allowing for a user-specified incident radiation spectrum rather than the monochromatic radiation now assumed. Finally, the best possible results would require material constants specific to the techniques used to fabricate the multilayer. This would require a great deal of effort since the measurement of most of the constants is not simple. For more information regarding material constants see Appendix B.

B. Improvements in experimental characterization

As with any experimental technique there is a wide range of possible improvements in these experiments. Ideally, a quasi CW source and a detector with nanosecond resolution over the time scale of the source would be used to measure the absolute reflectivity of the multilayer while a variable flux of up to approximately 1 GW/cm^2 of x rays irradiated the sample. But until such sources and detectors become available there are some minimal changes that should be made in future similar experiments. The most obvious of these suggestions is to correct problems with our apparatus such as the rotation of the streak camera film holder which precluded measurement of a shift in the Bragg angle. Also, as is shown by Fig. 12, the spectrum of x rays produced by the laser plasma varied dramatically with the energy of the laser pulse used to produce the plasma. The relative heights of the 930 eV and 950 eV lines were also observed to vary with the angle at which the plasma was viewed. Perhaps these effects could be better understood and used to enhance measurement capabilities. In future experiments efforts should be made to rearrange the apparatus to allow for the use of a second streak camera so that absolute reflectivity measurements can be obtained. This could be accomplished by directly observing the probe source intensity versus time

with one camera and observing the reflected intensity versus time with another camera. The direct measurements could then be used to normalize the reflected intensity measurements and obtain the reflectivity of the multilayer versus time. Similarly, some means of direct measurement of damage flux should be implemented. This could be done with a simple, compact, "pocket" spectrometer constructed to record the intensity of a few lines of interest. Film from the spectrometer could be exposed with a calibrated lamp as was done with the streak camera film so that flux values could be obtained. Finally, the range of multilayer materials tested should be expanded to include some of the combinations such as B_4C/C and TaC/C which have been predicted to respond more favorably to large x-ray fluxes.

C. Potential applications

The motives for robust multilayer studies have generally been limited to extending the capabilities of common multilayers in applications such as plasma diagnostics and x-ray laser research. The response of multilayers to large x-ray fluxes, however, suggests designs for devices previously available only at longer wavelengths. For example switching of powerful beams could be accomplished with a combination of a multilayer of known response and a slit.[31] Such as switch could operate either in a normally open or normally closed mode. Robust multilayers have also been proposed as Q-switching devices for x-ray laser cavities.[32]

APPENDIX A: ROMULS USER'S MANUAL

The code ROMULS has been written to be fairly simple to use. The most difficult part of using the code is obtaining the material constants for the constituents of the simulated multilayer. A list of constants for the materials simulated to date is given in Appendix B. The sources for these constants are references 33 through 42. These are a good starting point in a search for data for other materials. There are some numerical limitations in the code which determine the range of physical parameters which can be simulated. The current limitations are:

1. Maximum substrate thickness is 90,000 Å.
2. Layer thickness accuracy to 0.1 Å.
3. X-Ray wavelength between 1.24 Åand 124 Å.
4. Maximum number of layer pairs is 100.
5. Maximum number of time step frames is 21 (including $t = 0$.)
6. 2500 point maximum in plot files (product of number of time steps and number of angle steps.
7. The plot azimuth and altitude angles are currently set at 315° and 45° respectively.
8. The multilayer materials are not limited to atomic materials. Compounds may be entered by specifying a number of materials greater than 1 for either the even or odd layers or the substrate.

Given these limitations and the necessary data for the materials to be simulated, access to the XRAY MicroVAX is required. After successful login, a VAX DCL command file, ROMULS.COM will control execution of the codes. At the DCL $ prompt type @[GRAY.ROMULS]ROMULS.COM. If this is the first

simulation performed from the current account instructions will be given to set up logical names which determine from which directories ROMULS will obtain input files and to which directories it will write output files. Otherwise ROMULS will begin requesting input. At this point an input file may be specified or ROMULS will request the simulation parameters one by one. In either case the data is echoed to a file which may be used later as an input file. Indeed the simplest method of creating an input file is to run the code and enter the data as prompted. Once data entry is complete the option will be given to begin the simulation or save the batch file for later execution. Once execution has begun no further action is required. Upon completion of the simulation a plot of reflectivity vs. angle vs. time will be printed on the line printer and the data saved in the user-specified location for plotting on a wide range of devices.

Among the files written to output directory is a large log file which contains all of the output of code, not just the final plot. Much of the information in this file is self-explanatory, however, reading the log file can be confusing because of the volume of information presented. The most important information for the user is contained in the time-step dumps. At user-specified times (real time) the code writes vital physical and thermodynamic information about each layer in the multilayer to the log file. When reading these time-step dumps the following abbreviations will be encountered in the headings above the data for each layer:

X: position

V: velocity

I: zone number

T: temperature

RHO: density

P: pressure

STRESS X, STRESS Y: x,y "stress deviator" See reference 24.

Q: artificial viscosity

E: specific internal energy

RMFP: Rosseland mean free path

SUM MV: sum of the layer momenta from the surface

CS: sound speed

PH: phase (solid, liquid, etc.)

Given the data in the log file and the plotted data, interpretation of the results can begin. It should be noted that the plots alone can be misleading when evaluating the life of a multilayer since the multilayer may continue to exhibit reflectivity even though some or all of the layers have melted. A more realistic time-to-destruction must be determined by comparison of the plotted data and logged data. Although the multilayer may retain sufficient reflectivity in many cases substantial subsidiary reflection peaks arise. These limit the usefulness of the multilayer because they lead to difficulties in the interpretation of observed reflection peaks.

APPENDIX B: ROMULS INPUT DATA

Table 1 contains collected input data for a few materials. The sources for this data are references 33 through 42. These sources also contain data for many other materials. In general, the required constants for compounds may be more difficult to find than for elemental materials. When compiling materials data for input into ROMULS note that the units used by the code are cgs with temperature measured in electron-volts. Table 2 contains conversion factors for units commonly encountered in the literature. As will be noted from these references, the sources are collections of data for groups of materials; any one constant may not be the best available. If exceptional accuracy is required the extensive and scattered literature for each material should be consulted. Furthermore, remember that most of these constants have been determined at standard temperature and pressure.

In Table 1 the following abbreviations and symbols will be used: Z is the atomic number, A is the atomic weight, ρ is the density, T is the tensile strength, B is the bulk modulus, γ is the Gruneisen coefficient, θ_D is the Debye temperature, E_C is the cohesive energy, T_M is the melting temperature, H_o is the thermal conductivity, and α gives the temperature dependence of the thermal conductivity. The cohesive energy, also known as the zero temperature separation energy, is the energy required to separate 1 g of a substance from a solid sample and each other. The thermal conductivity is specified by the equation $H = H_o T^{\alpha}$. Again, the quantities are specified in the cgs system of units with temperature specified in eV.

Table 1. ROMULS Material Input Data

Material	C	W	WC	Mo	Si
Z	6	74	74/6	42	14
A	12.01	183.85	94.19	95.94	28.08
ρ	2.26	19.3	14.97	10.2	2.32
$T \times 10^8$ †	1.62	48.3	100.	52.0	300.
$B \times 10^{11}$	3.4	29.7	36.1	27.2	9.88
γ	0.24	1.77	1.5	1.65	0.57
θ_D	0.1335	0.0334	0.0532	0.0325	0.0596
$E_C \times 10^{11}$	5.92	0.454	0.463	0.685	1.6
T_M	0.3353	0.3147	0.2708	0.2488	0.1452
$H_o \times 10^{10}$	0.3482	23.2	5.80	17.4	23.2
α	2	−0.5	2	−0.5	−1

Material	V	Ti	TaC	B	Li
Z	23	22	73/6	5	3
A	50.94	47.88	192.96	10.8	6.94
ρ	6.10	4.53	14.48	2.34	0.533
$T \times 10^8$	107	69	200	1.62	0.27
$B \times 10^{11}$	16.2	10.5	34.5	17.8	1.36
γ	1.55	1.33	1.5	1.8	0.92
θ_D	0.0336	0.0327	0.0494	0.117	0.0386
$E_C \times 10^{11}$	1.00	0.98	0.369	5.06	2.3
T_M	0.1877	0.1672	0.362	0.198	0.0391
$H_o \times 10^{10}$	3.48	2.9	4.64	0.35	0.058
α	0	−0.5	0.5	2	0.5

† This means multiply the table value by 10^8

Table 2. Conversion factors

To convert from	To	Multiply by
Pa	$\frac{\text{dynes}}{\text{cm}^2}$	10
$\frac{\text{MJ}}{\text{kg}}$	$\frac{\text{ergs}}{\text{g}}$	10^{10}
$\frac{\text{MJ}}{\text{kg}}$	$\frac{\text{cal}}{\text{g}}$	239
$\frac{\text{W}}{\text{cm K}}$	$\frac{\text{erg}}{\text{cm sec eV}}$	1.16×10^{11}
Mbar	$\frac{\text{dynes}}{\text{cm}^2}$	1.01×10^{12}
$\frac{\text{kcal}}{\text{mole}}$	$\frac{\text{ergs}}{\text{g}}$	$\frac{1}{\text{A}} \times 4.184 \times 10^{10}$ †
psi	$\frac{\text{dynes}}{\text{cm}^2}$	6.9×10^4
$\frac{\text{kg}}{\text{mm}^2}$	$\frac{\text{dynes}}{\text{cm}^2}$	9.81×10^7
$\frac{\text{kg}}{\text{cm}^2}$	$\frac{\text{dynes}}{\text{cm}^2}$	9.81×10^5
K	eV	8.62×10^{-5}
$\frac{\text{cal}}{\text{mole K}}$	$\frac{\text{ergs}}{\text{g eV}}$	$\frac{1}{\text{A}} \times 4.85 \times 10^{11}$ †
gram − atom	mole	1

† A is the atomic weight.

References

1. J. DuMond and J. P. Youtz,*J. Appl. Phys.* **11**, 357 (1940).

2. R. M. Bionta, *Appl. Phys. Lett.*, **51**(10), 725 (1987).

3. Andrew M. Hawryluk, Natale M. Ceglio, and Daniel G. Stearns, in *Multilayer Structures and Laboratory X-Ray Laser Research*, Ed. Ceglio and Dhez, Proc. SPIE **688**, p. 81 (1986).

4. G. Schmahl, D. Rudolph, B. Niemann, in *High Resolution Soft X-Ray Optics*, Ed. E. Spiller, Proc. SPIE **316**, p. 100 (1981).

5. N. M. Ceglio, D. P. Gaines, J. Trebes, A. M. Hawryluk, D. G. Stearns, G. L. Howe, in *Multilayer Structures and Laboratory X-Ray Laser Research*, Ed. Ceglio and Dhez, Proc. SPIE **688**, p. 44 (1986).

6. R. Marmoret, I. Mosnier-Thoumas, M. Pirocchi, R. Barchewitz, J. Susini, R. Rivoira, R. Philip, in *Multilayer Structures and Laboratory X-Ray Laser Research*, Ed. Ceglio and Dhez, Proc. SPIE **688**, p. 184 (1986).

7. Bryan G. Peterson, "Establishment of the Feasibility of Constructing a Soft X-Ray Mach-Zender Interferometer", Report on Department of the Army contract DASG60-87-C-0050, 1987 (unpublished).

8. Troy W. Barbee Jr., *Optical Engineering* **25**(8), 898 (1986).

9. James H. Underwood and David T. Atwood, *Physics Today*, April 1984, p. 44.

10. L. Golub, E. Spiller, R.J. Bartlett, M.P. Hockaday, D.R. Kania, W.J. Trela, R. Tatchyn, *Applied Optics* **23**(20), 3529 (1984).

11. E. Ziegler, Y. Lepetre, Ivan K. Schuller, E. Spiller, *Appl. Phys. Lett.***48** (20), 1354 (1986).

12. H. Nakajima, H. Fujimori, M. Koiwa, *J.Appl.Phys.* 63(4), 1046 (1988).

13. D. Kohler, J. L. Guttman, B. A. Watson, and Michael Gerassimenko, *Rev. Sci. Instrum.***56** (5), 812 (1985).

14. Y. Tagaki, S. A. Flesa, K. L. Hart, D. A. Pawlik, A. M. Kadin, J. L. Wood, J. E. Keem, and J. E. Tyler, in *Applications of Thin Film Structures to Figured X-Ray Optics*, Ed. Gerald Marshall, Proc. SPIE **563**, p. 66 (1985).

15. J. M. Thorne, L. V. Knight, B. G. Peterson, R. T. Perkins, K. J. Gray, in *Multilayer Structures and Laboratory X-Ray Laser Research*, Ed. Ceglio and Dhez, Proc. SPIE **688**, p. 139 (1986).

16. D. Allred, personal communication.

17. M. Y. P. Hockaday, *An Experimental Measurement of Metal Multilayer X-Ray Reflectivity Degradation due to Intense X-Ray Flux*, Los Alamos National Laboratory LA-10989-T, Ph.D. Thesis, New Mexico State University, Las Cruces, New Mexico (1987).

18. M. Y. P. Hockaday, Los Alamos National Laboratory LA-10989-T, 1987, p. 176.

19. M. Y. P. Hockaday, Los Alamos National Laboratory LA-10989-T, 1987, p. 181.

20. Jim Swain, personal communication.

21. R. M. More, K. H. Warren, Z. Zinamon, in *Multilayer Structures and Laboratory X-Ray Laser Research*, Ed. Ceglio and Dhez, Proc. SPIE **688**, p. 134 (1986).

22. D. R. Kania, in *Multilayer Structures and Laboratory X-Ray Laser Research*, Ed. Ceglio and Dhez, Proc. SPIE **688**, p. 157 (1986).

23. B. L. Henke, P. Lee, T. J. Tanaka, R. L. Shimabukuro, and B. K. Fujikawa, *Atomic Data and Nuclear Data Tables* **27** (1), (1982). Table converted to computer readable form by J. Auerbach.

24. S. L. Thompson and H. S. Lauson, Sandia Laboratories SC-RR-71 7013, 1972.

25. K. K. Shih, D. A. Smith, J. R. Crowe, *J. Vac. Sci. Tech. A*, **6**(3), 1681 (1988).

26. J. H. Underwood and T. W. Barbee Jr., *Applied Optics* **20** (17), 3027 (1981).

27. B. G. Peterson, H. K. Pew, L. V. Knight, D. P. Gaines, in *Soft X-Ray Optics and Technology*, Ed. Kohl and Schmahl, Proc. SPIE **733**, p. 405 (1986).

28. A. Zigler, M. Kishenevsky, M. Givon, E. Yarkoni, B. Arad *Phys. Rev. A* **35** (10), 4446 (1987).

29. J. J. Rocca, D. C. Beethe, M. C. Marconi *Optics Letters* **13** (7), 565 (1988).

30. B. G. Peterson, "Development of a Compact, Inexpensive X-Ray Laser Driver", Funded proposal to the National Science Foundation, June, 1988.

31. J. S. Wark, A. Hauer, J. D. Kilkenny, *Rev. Sci. Instrum.* **57** (8), 2168 (1986).

32. James M. Thorne, personal communication.

33. A Periodic Table of the Elements such as Sargent-Welch # S-18806.

34. Chemical Rubber Co. Handbook

35. *T-4 Handbook of Material Properties Data Bases*, edited by Kathleen Holian, Los Alamos Scientific Laboratories LA-10160-MS, Nov. 1984.

36. Karl A. Gschneidner Jr., in *Solid State Physics: Advances in Research and Applications*, edited by Frederick Seitz and David Turnbull, (Academic Press, 1964), Vol. 16, pp. 275-426.

37. *X-Ray Data Booklet*, edited by Douglas Vaughan, (University of California, Lawrence Berkely Laboratory Center for X-Ray Optics, 1985).

38. D. F. Miner, *Handbook of Engineering Materials*, (Wiley, Canada, 1955).

39. *Thermophysical Properties of Matter*, Vol. 1,2 (IFI/Plenum, N. Y. 1970).

40. *Refractory Materials*, Vol. 2, "Refractory Carbides", (Academic, 1967).

41. *Refractory Materials*, Vol. 7, "Transition Metal Carbides and Nitrides", (Academic, 1967).

42. *Physical Properties of Solid Materials*, (Pergamon, London, 1954).

Simulated and Measured Response of Robust
Multilayer X-Ray Reflectors

Kevin J. Gray
Department of Physics and Astronomy
Ph.D. Degree, August 1989

ABSTRACT

Some recently proposed applications of multilayer x-ray reflectors expose the multilayer to damaging fluxes of x rays. This paper reviews proposed damage mechanisms and material selection techniques aimed at reducing the effects of damaging fluxes. Experiments were performed to measure the response of tungsten/carbon, and tungsten carbide/carbon multilayers to laser plasma x-ray fluxes of approximately 200 MW/cm^2. These multilayers were found to maintain significant reflectivity for at least 1 ns. A computer program ROMULS has been developed which will predict the reflectivity vs. angle vs. time behavior of multilayers in high flux applications. A description of this program is given. Comparison of the simulations and experimental results indicate that ROMULS underestimates the useful lifetime of multilayers by a factor of two or three. Suggestions for improvements in experimental and simulation techniques are given. A detailed guide for operation of ROMULS is presented.

COMMITTEE APPROVAL:

Larry V. Knight, Committee Chairman

David D. Allred, Committee Member

William E. Dibble, Committee Member

Daniel L. Decker, Department Chairman